Effects of rig tension on sailing yacht performance

Internship report

Friso Bergsma
March 2012

Engineering Fluid Dynamics – University of Twente
Yacht Research Unit – University of Auckland

Acknowledgements

I would like to thank the University of Auckland and the Yacht Research Unit for hosting me during my internship.

First of all I would like to thank Peter Richards and David Le Pelley. I thank Peter Richards for creating the opportunity to spend my internship at the Yacht Research Unit and giving valuable feedback and suggestions for the direction of research. I thank David for supervising me at the wind tunnel. His help with the setup of the experiments, the experiments themselves and analyzing and interpreting the data is much appreciated.

I would like to thank Dale Morris for his help during the project. The code he developed during his graduation project proved very valuable for my research project. His patient explanations were very helpful.

I thank Dario Motta working together on the pressure measurement system and his help with my project.

I thank Dan, Alex, Pieter, Giovanni, and Jean Sebastian for helping with the full scale testing and for making my time at the Yacht Research Unit to the great time it was!

Friso Bergsma

Auckland, March 2012

Table of Contents

1. Introduction

When yacht racing, the aim is always to go faster: faster than the previous time, faster than the opponent, faster than someone owning an identical boat. When a new class is introduced, there's often an idea about the speed potential of a yacht. This combined with general rules for trimming a boat make that the new crew knows to sail the new yacht as fast as possible

With time the experience with the new yacht increased and often detailed trim guides are written. For other classes dock talk is the way trim details are shared from one yacht to another. The yacht gets 'mature' and all details about the optimum trim are gained via experience.

The Stewart 34 is such a mature type of yacht. It was designed in 1958 by Bob Stewart, and the first yacht was launched end of 1959 and since that time at total of 63 yachts have been launched. They are still being raced very competitively, mainly from Auckland. Known worldwide because the 'Citizen Watch Match racing series' the yachts have been sailed by the best sailors of the world.

During these years of competitive sailing is was noticed that many of the top boat have very slack cap shrouds causing a big sideways deflection of the mast(top). The believe is that the increase in performance is caused by these slack cap shrouds.

The research presented in this report was conducted to find out if the performance actually increases due to slack cap shrouds, and what causes this increase in performance. Full scale tests were performed on the Stewart 34 'Pride'. Aerodynamic forces were determined and compared for different shroud settings.

The second chapter of this report gives an introduction to the theory behind sailing and force generation of sails. Experiments that were performed for this research are described in chapter three. The used equipment, conditions and testing procedure are described.

The analysis of the data acquired with these experiments is described in chapter four. Performance indicators are described, the way aerodynamic forces and gap width are determined, is described. The results from processing the data are presented in chapter five. A verification of the measured forces with literature values is performed and the data is used to test a series of hypothesizes. The conclusion of these results follows in chapter 6.

2 Theory

2.1 Force generation

Sailing yachts are complex machines that act on the interface of two fluids: water and air. Their motions are determined by the balance of the forces generated by the sails in the air domain and by the hull and appendages in the water domain.

The aerodynamic forces can be distinguished in lift and drag components, but more conveniently, they are split in driving and heel force, which are the component in the direction of the centerline and the component lateral to the centerline respectively (see figure 2.1).

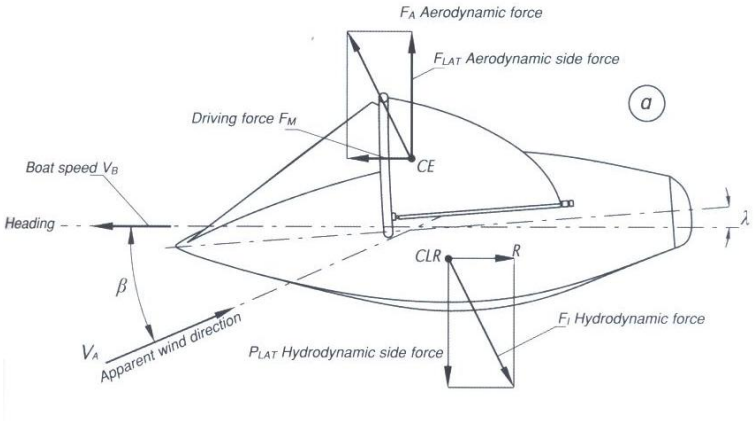

Figure 2.1: driving force and heel force as components of the aerodynamic force.

Sails can be described in a way similar to foil sections. However, it should be notices that the shape varies along the span of a sail, and sails usually have almost no thickness. The chord is the straight line between leading edge and trailing edge, or luff and leech of the sail. Camber is the perpendicular distance between chord and the foil. The draft is the chord wise position of the maximum camber (figure 2.2).

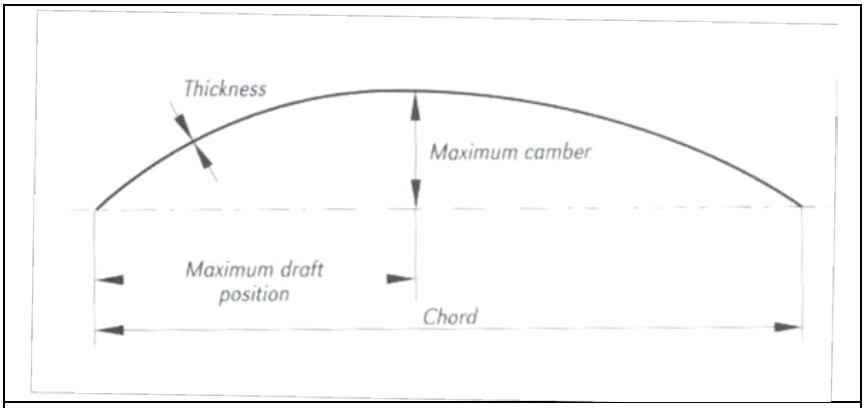

Figure 2.2: definition of sail shape.

Force is generated by sails in the same ways wing do: by generating a pressure difference over a surface. The generation of lift is explained by Gentry (2006). The airflow around a flat plate is used to illustrate the generation of lift. For the non viscous case the streamlines are shown in figure 2.3 This is the non lifting solution, also known as D' Alembert paradox. However, air is viscous, and the flow should confirm to the Kutta condition, which states that a body (e.g. a flat plate, or a sail) creates a circulation around itself, strong enough to hold the rear stagnation point at the trailing edge. This circulation around the plate creates the flow field shown in figure 2.4. There is a high speed area on top of the plate and a low speed area at the bottom. Bernoulli tells us that this gives a low pressure area on top of the wing and a high pressure area at the bottom. The theory applied for a flat plate also applies for other sections such as sails.

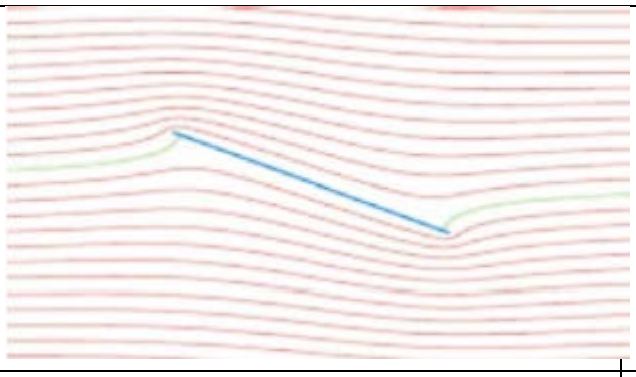

Figure 2.3: non-lifting flow around plate.

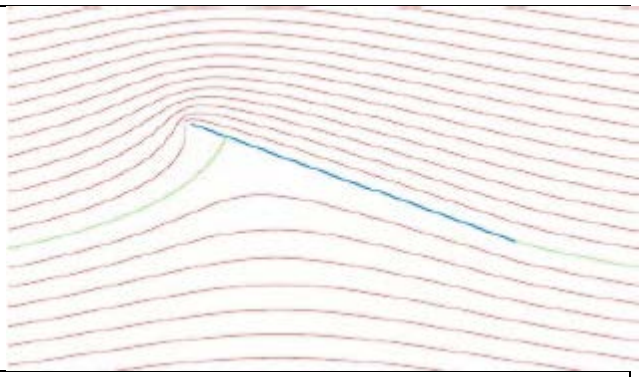

Figure 2.4: Lifting flow around plate.

2.2 Interaction between main sail and head sail

The effect of interaction between head sail and main sail is shown in figure 2.5. This figure shows the stagnation lines for the head sail only (blue), the main sail only (green) and for the combination of both sails (red). The presence of the main sail causes an upwash to the head sail, because the main sail deviates the flow arriving towards it. The effect of the headsail on the main is a downwash (the stagnation line of main shifts towards windward). This is a unfavourable deviation, but in also causes a smaller variation in velocity, thus pressure. This means there is a smaller risk of boundary layer separation, or stall of the main sail. For overlapping head sails the downwash might cause back winding on the main sail (Fossati, 2007), (Gentry, 1973).

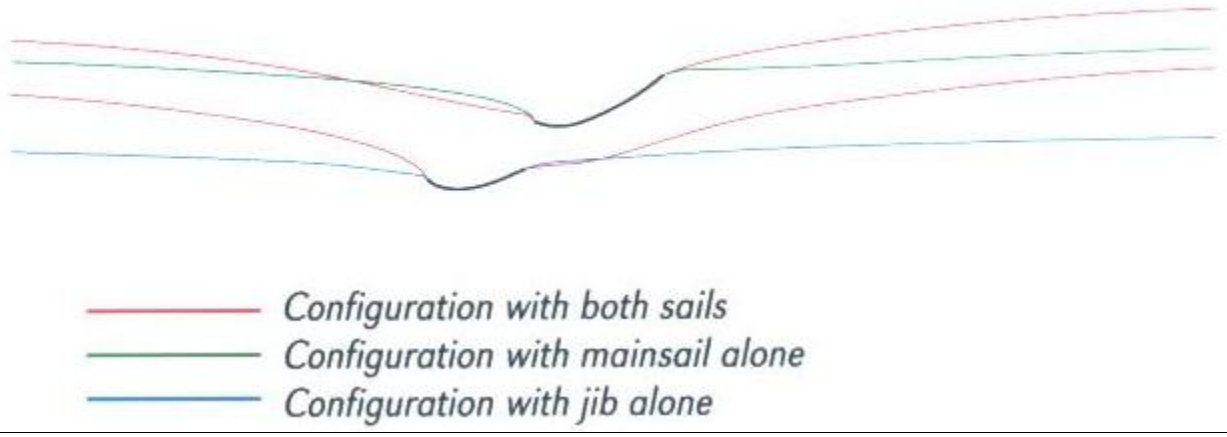

Figure 2.5: effect of interaction on the flow around sails.

2.3 Gap between main sail and head sail

The interaction between main sail and head sail only pays off if the head sail is allowed to perform effectively. This is determined by the gap width between the head sail and the main sail. It is well known that the trim angle of the head sail, or the distance between head and main sail is very important to the overall performance of the yacht.

Experiments in the wind tunnel at the University of Southampton show that if the slot between the head sail and main sail is increased, the driving coefficient can be increased significantly, while reducing the heeling force (Marchaj, 1964).

There are limitations to the possibilities to shape the gap width, but factors that control the shape of the gap, according to Marchaj are:

- Position of the fairleads
- Point of attachment of tack of head sail
- Trim of main sail and head sail
- Sag in the forestay
- Planform of the foresail
- Camber of mainsail and foresail

For the Stewart 34 the tension on the cap shrouds can be added to this list of factors that control the gap width.

2.4 Aerodynamic force deduction on full scale

For determining the aerodynamic forces produced by the sails, Force Evaluation via Pressures and VSPARS (FEPV) is used. The shape of the sail is captured at full scale using the VSPARS system, yielding the shape of the sail at three different heights of the sail (figure 2.6). The shape of the sail is extrapolated using splines and assumptions of the position of the top and the bottom of the sail.

The pressure differences are measured at 24 discrete positions per sail, close to the positions where the shape of the sail is captured. Using linear extrapolation the pressure distribution over the sail is determined. (figure 2.7). The pressure differences and the area of each cell is now known, making it possible to determine the force components using the following equation (Le Pelley, Morris & Richards, 2012):

$$\hat{F} = \sum P_{ij} \cdot A_{ij} \cdot \boldsymbol{n_{ij}}$$

Where P_{ij} is the pressure difference, A_{ij} is the cell area and $\boldsymbol{n_{ij}}$ is the unit normal vector for cell(i,j).

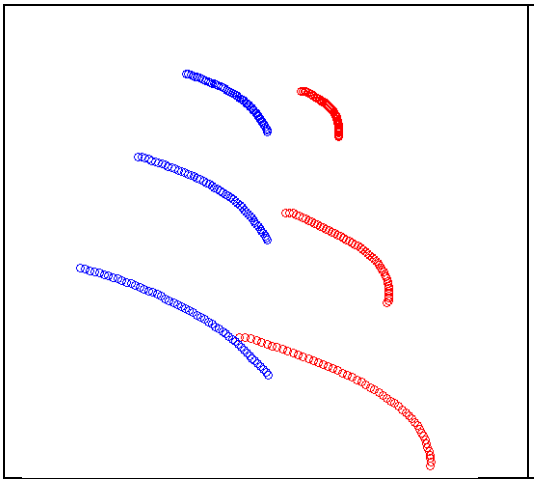

Figure 2.6: shape of the sails at different heights.

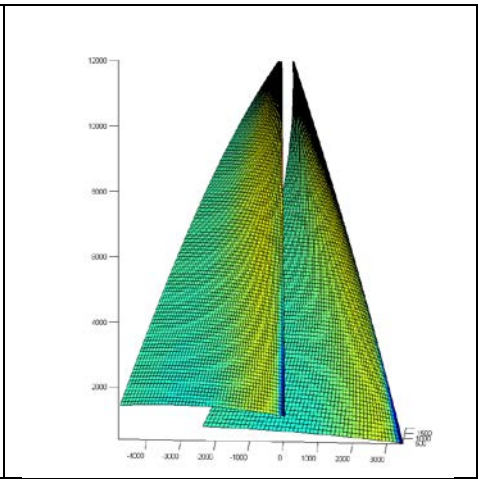

Figure 2.7: pressure distribution over sail.

3. Experiment

The tests were performed in the Tamaki strait (figure 3.1) aboard the Stewart 34 'Pride' owned by David Le Pelley. Typically it takes a day to install and prepare all equipment aboard and one day to perform the tests. A description of the experiments follows below. First the equipment is detailed. Then the conditions at the day of the experiment are detailed and then the test procedure is described.

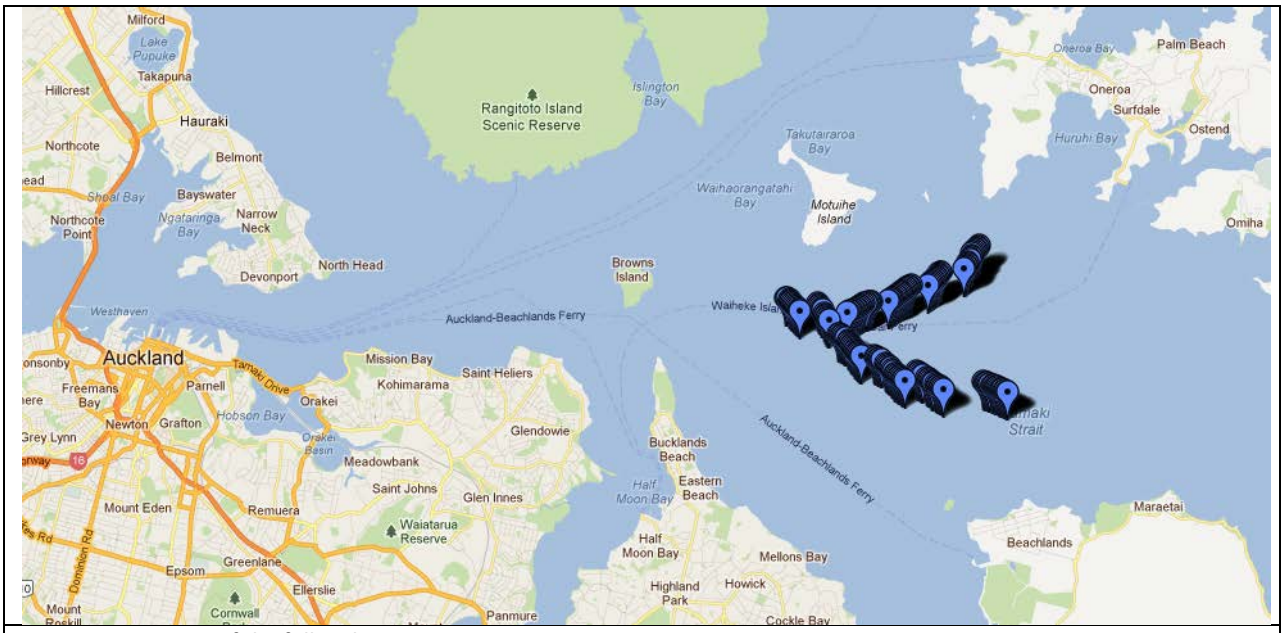

Figure 3.1: Location of the full scale experiments.

3.1 Equipment

In order to monitor the performance and behaviour of the Stewart 34 as detailed as possible, a variety of measurement devices were used. Some equipment was already installed at the yacht such as the log to measure speed trough the water, but most equipment is installed for the purpose of the experiment.

Pressure Measuring System

The pressure measuring system is developed by David Le Pelley and Dale Morris (Morris, 2011). For each sail it consists of 24 pressure taps placed at three different heights. The pressure taps measure a pressure difference over the sail. To be able to measure the pressure difference a hole is burnt in the sail at the location of each tap using a soldering iron. The taps are attached to the starboard side of the sail with double sided tape. To secure them further and to improve the aerodynamics of the sail with the pressure taps, they are covered with a piece with sailing cloth. These patches had a perforation at the position of the tap as well.

To be able to record the pressure profile along the chord accurately, four pressure taps are placed in the first 25% of the chord. This is the part of the chord where high pressure gradients occur. The first pressure tap is placed as close to the leading edge as possible. The locations of the taps are tabulated in table 3.1-2 for the main and the head sail.

Stripe	Bottom	Middle	Top
Height from tack	2780	5502	7690
Tap 1 [x/c]	0.031	0.029	0.037
Tap 2 [x/c]	0.101	0.101	0.075
Tap 3 [x/c]	0.147	0.144	0.109
Tap 4 [x/c]	0.198	0.194	0.144
Tap 5 [x/c]	0.25	0.245	0.213
Tap 6 [x/c]	0.448	0.435	0.362
Tap 7 [x/c]	0.698	0.68	0.566
Tap 8 [x/c]	0.946	0.917	0.779

Table 3.1: location of the pressure taps in main sail.

Stripe	Bottom	Middle	Top
Height	3458	6544	9708
Tap 1 [x/c]	0.01822	0.0259	0.0614
Tap 2[x/c]	0.04784	0.0481	0.07456
Tap 3 [x/c]	0.08656	0.0887	0.11842
Tap 4 [x/c]	0.12301	0.1257	0.15789
Tap 5 [x/c]	0.24146	0.244	0.28947
Tap 6 [x/c]	0.47153	0.4769	0.52632
Tap 7 [x/c]	0.70159	0.7135	0.77632
Tap 8 [x/c]	0.93052	0.9501	0.95614

Table 3.2 location of the pressure taps in the head sail.

Each pressure tap is equipped with a amplifier to amplify the analogue output to a signal in the $\pm$ 2.5 V range. The eight pressure taps at one stripe are connected to a ribbon cable. At the luff these ribbon cables are connected to a A/D converter which converts the analog signal to a digital signal. A ribbon cable along the luff of each sail connects the A/D converters to a microcontroller which is connected to the data acquisition computer (Morris, 2011).

Calibration of the pressure transducers is required for accurate measurement of the pressures. Using a pressure calibrator three reference pressures were applied for which the bit data were measured. These were used to determine a gradient m. this gradient was determined within on to three days before the experiments. The bit value was determined as well for situation in which the pressure difference is zero. This is called the zero reading θ_{zero}. These readings are done as short as possible before the experiment, i.e. on the day of the experiment out on the water. The sails were covered with sail covers and the apparent wind speed was minimized in order to minimize pressure differences.

With the gradient and the zero value known, the pressure could be determined from the bit reading using the following relation:

$$p = \frac{(\theta - \theta_{zero})}{m}$$

VPSPARS

For measuring the shape of both head and mainsail and the position of the rig the VSPARS system is used. This system uses inexpensive off-the-shelf digital cameras and is developed by David Le Pelley and Owen Modral. It uses three deck mounted cameras that capture images of the shape of the sails. The sails are equipped with horizontal stripes at different heights. These stripes have a high contrast colour, orange in the case of the Pride, for easy recognition. Both sails have 3 stripes, approximately at 1/4th, 1/2th and 3/4th of the height of the sail.

The software recognizes the stripes and determines their position and shape. To be able to do so it requires the x, y, and z position of the camera relative to the datum (aft face of the mast at deck height), the height of the stripes along the luff of the sail and the angle of the camera.

For this experiment discrete samples of the sail shape are taken, up to approximately 10 per minute. For each sample an output file is generated. This states the x, y and z position for several points per stripe. For each stripe additional data such as entry angle, exit angle, depth, draft, sag, bend and twist are given as well.

GPS

For the measurement of the position of the Pride an external GPS was connected via USB to the data acquisition system. Data output was in the NMEA format. The Speed Over Ground (SOG) was extracted from these data files.

Boat instruments

The boat instruments were connected to the data acquisition system as well. Data output was in the NMEA format. The data files provided the Heading, Apparent Wind Angle (AWA) and Apparent Wind Speed (AWS).

Inertial Measurement Unit

The motions of the mast top are measured with the inertial measurement unit of the type Razor 9DOF AHRS produced by Sparkfun. It was used for determining the heel angle of the yacht.

Sonic anemometer

A sonic anemometer was placed at the top of the mast for measurement of the components of the wind speed. With these three components the wind direction and speed can be determined. The sonic anemometer is of the type 81000 produced by R.M. Young USA.

Data acquisition system

The data was recorded to two different pc's from previous experience was learned that a single computer of the type fit-PC2 was not powerful enough to cope with all connected equipment. Therefore a second laptop was used. One pc was dedicated to run the VSPARS system, the other was dedicated to record data from the other equipment. The times at the pc's were set equal to make sure the correct VSPARS data could linked to the corresponding data from other equipment

3.2 Conditions

Good and steady weather are very important for the experiments. The taps are not waterproof so it should be a rain free day. Due to the size of the sails equipped with pressure taps light winds are required. To have comparable results of the experiments the windspeed and direction should not change too much. Experiments were performed at the 9th of February 2012 between approximately 11am and 3pm. This day fulfilled these requirements, being a clear summer day with a reasonable constant breeze throughout the day

Location

The experiments were performed in the Tamaki Strait, south of Motuihe Island. Location of the runs are shown in figure 3.1. The first runs were done sailing in a north eastern direction on port tack. There are four pieces of line distinguishable in this direction. Each stretch corresponds to one rig tension setting. Within each stretch three runs were performed, with different headings to the apparent wind. At approximately 2pm runs on port tack were completed. The next series of runs were made in north western direction.

Weather

The 9th of February was a clear and dry day with a constant light breeze between 11 and 15 knots. The wind direction was North North Westerly with small variations during the day. The wind speed and direction are shown in figure 3.2. These values are the averages of the measured values over a run, which takes typically about one minute. Small variations in speed and direction are due to gusts. During the runs on port tack (until 2pm) the speed is constant. During the tests at starboard tack the wind first increases slightly to decrease for the last few runs.

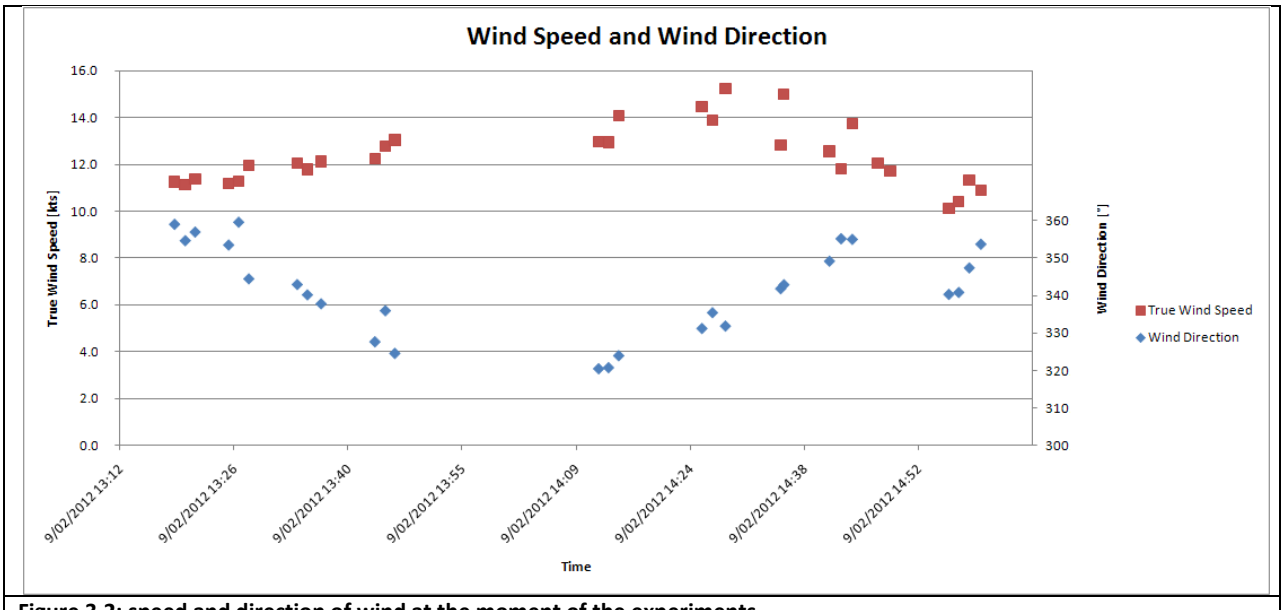

Figure 3.2: speed and direction of wind at the moment of the experiments

Tide

High tide occurred at 8:18am in the Hauraki golf at the 9th of February (LINZ, 2011). Due to the full moon of the 7th of February this is a spring tide. This is suboptimal, but a part of full scale testing that is hard to

influence. Using tidal diamonds in the chart the strength and direction of the tide has been determined. They are shown in table 3.3

Time	Speed [kts]	Direction [°]
1:18pm	0.3	056
2:18pm	0.2	059

Table 3.3: Strength and direction of tide at the moment of the experiments.

This means that on the port tack, the yacht experiences 0.3 knots of current in the sailing direction. On the starboard tack the yacht is set aside to lee by the current with a speed of 0.2 knots.

3.3 Test Procedure

A series of experiments takes typically two days, where the first day is allocated for setting up, and the second day is used for the actual experiments and gathering data.

On the 8th of February, the equipment was brought to the yacht and installed. The sonic anemometer is placed at the mast top together with the IMU. This needs to be aligned with the longitudinal axis of the yacht, which is done visually. Next the three VSPARS cameras are mounted at their positions and aimed to be able to view the whole sail. The cruising sails are replaced with the sails that are equipped with VSPARS-stripes and the pressure taps. The system, including GPS, boat instruments is wired up with the data acquisition pc. This gives the possibility to check if all data is acquired correctly. The cap shrouds were set to a light tension the distance between the mast top and deck spreaders was measured to have equal values for port and starboard. By visual inspection was checked that the mast was straight.

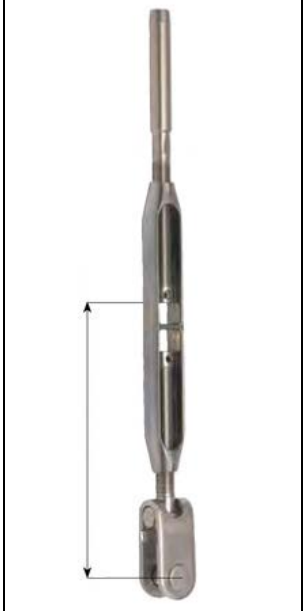

Figure 3.3: measured distance.

The 9th of February was spent doing the actual experiments. The data system was checked again and zeroes were determined for the pressure taps of both main and head sail. A first set of zeroes was determined in the harbor. A second set of zeroes was determined out at sea, as short as possible before the actual tests.

The first set of runs was done on port tack. The current cap shroud tension was used for the first series of runs. With these settings a standard trim was defined for this tack. Sheets, traveler, fairlead and backstay were marked, to be able to set the sails back to this configuration easily.

For a tension, three different headings were tested:

- VMG: steering for optimal speed upwind
- Pinching: steering few degrees higher than VMG
- Footing: steering few degrees lower than VMG

Measurements would typically take about one minute, with about the same time between two runs of different headings. After runs were performed for all three headings the cap shroud tension was adjusted by adjusting the turnbuckle. First the cap shrouds were eased. The last cap shroud setting was tight. The distance D between the base of the cap shroud thread and the pin was measured (see figure

3.3). The four different settings for the cap shrouds and their accompanying distances are tabulated in table 3.4. For each of these settings the procedure as described above was repeated.

setting	$D\ [mm]$
Tight	205
Medium	220
Slack	240
Fully slack	252

Table 3.4: shroud settings.

After the last run on port, the yacht tacked and the measurements were repeated for the starboard tack. This time the first series of experiments were done with tight cap shrouds, easing them after data for all three headings were recorded. The standard sail trim was defined at the first run. This also means that the standard sail trim on starboard tack was defined with the cap shrouds set tight, as opposed to medium for the standard sail trim for port. The same procedure as done for the port tack was repeated for starboard.

3.4 Limitations

Due to the nature of full scale tests there are some limitations. Factors that might influence the experiments and the acquired data, include:

- Tide: this might cause asymmetry between measurements at port and starboard, e.g. in wind speed.
- Waves: To a certain limit are waves regularly, but the variations can cause variations in boat speed. If abnormal big waves were encountered, e.g. caused by ships runs would be aborted and redone in more constant conditions. Yet it remains inevitable that waves were not the same during all runs.
- Variations in wind speed: The wind speed varies during the day, though the wind was reasonable constant, small variations are part of full scale measurements and influence driving force, boat speed and sail shape

Effort has been made to set up the experiment as optimal as possible, yet there are limitations to the setup that should be noted:

- The mast: this was assumed to be rigged symmetric. This is inspected visually, but small differences in shape or shroud tension might be possible.
- Alignment with yachts CL: the IMU, sonic anemometer and the wind meter of the boat instruments are assumed to be aligned with the yachts centre line. Small deviation from this axis might cause asymmetry in measured wind and heel angles.
- Calibration of VSPARS: because the orientation of the cameras were slightly changed after leaving harbor, the pictures that were taken at the dock could not be used to define a zero position of the mast. Pictures that were taken during sailing were used instead. The mast might have a slight bend and sag in these pictures, that influence the post processing of mast bend and sag

- Calibration of IMU: The inertial measurement unit needs to be zeroed before measurements. This was done at the dock, where the boat is assumed to be upright. Because of a unreliable connector the IMU lost power during measurements a few times. Recalibration was necessary. This was done by sailing downwind and keeping the yacht as upright as possible, but small deviations are possible.
- Calibration of the pressure taps: zero measurements are done in the harbor and when at the water. The sails were covered to prevent wind from flowing over the taps and thus causing a pressure difference. This method is not flawless and might have caused asymmetry in the pressure measurements.

4. Analysis

In order to determine the cause of the increase in performance, first it needs to be analyzed if there is a performance increase due to the increased length of the cap shrouds (i.e. less tension)A relation between several performance indicators and the increased length of the cap shrouds (i.e. less tension) is sought for.

Secondly the cause of the increase in performance needs to be analyzed. The increase is thought to be caused by the increased separation between main and headsail. A relation between the slot width and performance indicators is sought for.

This chapter describes the possible relations and the methods that are used to analyze the data that is acquired during the experimental phase.

4.1 Hypothesis

Since the increased performance is assumed to be primarily upwind, an increase in performance can be defined in two possible ways. The goal of upwind sailing is to sail to windward as fast as possible. This can be done in two different manners, either by going faster, i.e. increasing the boat speed, or by sailing closer to the wind, i.e. decreasing the apparent wind angle (AWA). This leads to the first two hypothesizes:

Yachts of the type Stewart 34 are able to sail faster upwind with slack cap shrouds.

Yachts of the type Stewart 34 are able to sail closer to the wind with slack cap shrouds.

Boat speed depends to several variables. Of which some can be controlled, but some others not, for example sea state, wind speed and apparent wind angle. To be able to compare performance independent of the sea state, only the aerodynamic forces are taken account. This is done by determining the forces generated by the sails. To take account for variations in wind speed and AWA the force coefficient in the direction of the wind is determined. This value is called the corrected force made good coefficient, or $CF_{x,MG,\eta}$. This leads to the third hypothesis:

Yachts of the type Stewart 34 are able to achieve a higher $\boldsymbol{CF_{x,MG,\eta}}$ with slack cap shrouds.

In the above described situation, an increase in $CF_{x,MG,\eta}$ does not necessarily lead to increase in performance, since the hydrodynamic part is omitted. To get a more complete idea of the performance is it relevant to take the heeling moment in account as well. A high heeling moment leads to big angles of heel, which is often related to an increased drag. A performance indicator that takes these effects in account is the force made good coefficient divided by the heel moment made good. This indicator is denoted by $\frac{CF_{x,MG,\eta}}{CM_{x,MG,\eta}}$. Here the heel moment coefficient is determined in the same way as the force coefficient. Taking account for the heeling forces leads to the fourth hypothesis:

Yachts of the type Stewart 34 are able to achieve a higher $\boldsymbol{\frac{CF_{x,MG,\eta}}{CM_{x,MG,\eta}}}$ with slack cap shrouds.

The cause of the increased performance of the Stewart 34 with slack cap shrouds is thought to be due to a bigger separation between the headsail and the mainsail. A bigger gap width can be achieved by an increased sideways deflection of the mast or sag. This leads to the fifth hypothesis:

The sag of the mast top of a Stewart 34 increases with increasing slack cap shrouds.

To verify that the gap width actually increases with increasing slack cap shrouds the sixth hypothesis is:

The gap width of a Stewart 34 increases with increasing slack cap shrouds.

The seventh hypothesis is to verify that an increase in gap with leads to an increase in performance:

Yachts of the type Stewart 34 are able to achieve a higher $CF_{x,MG,\eta}$ with a bigger gap width.

4.2 Analysis method

In this paragraph is described how the data is analyzed that was acquired during the experimental phase. The data is processed using MATLAB and Microsoft excel. The results are shown in the next chapter.

For every run that was recorded a set of data files is available. This set containing the following types of data files:

- Boat data
- GPS data
- IMU data
- Head sail pressure data
- Main sail pressure data
- Sonic anemometer data
- Begin and end time of a run

Every few seconds a picture of the sail shape was taken, which was processed by the VSPARS software. Using the timestamps these files were connected to the corresponding runs.

Preprocessing VSPARS data

The data of the sail shape, that was available for every picture, was post processed using VSPARS. Pictures that were taken during a run were selected. These pictures were checked manually, and adjusted where the software was not able to recognize the sail shape. To improve the determined mast shape (bend and sag) extra points were added near the top of the mast in the pictures of the mainsail. (see figure 4.1-2). When the pictures were satisfactory, averages of the sail shape were taken. These files are the input that is used to determine the mast shape, gap width, and the sail shape, which is required to deduct the forces components produced by the sails.

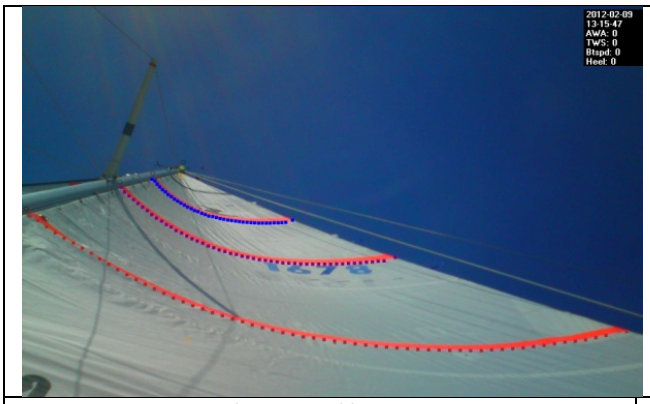

Figure 4.1: stripes as determined by VPSPARS.

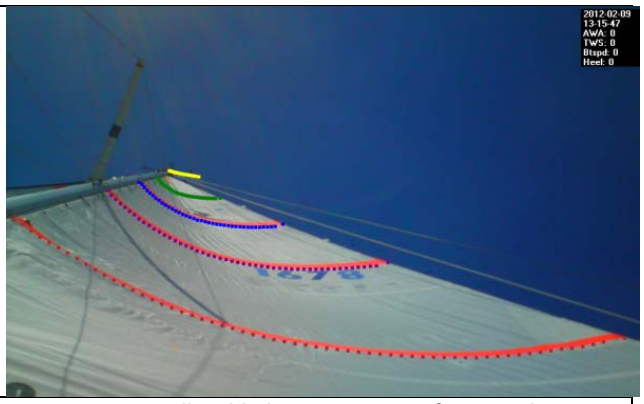

Figure 4.2: manually added stripes on top of main sail.

Structuring data

As stated above, a big amount of data is generated which is spread over a several files. To make the acquired data more accessible, the first step was to extract the relevant data from the data files and structure it in an easy accessible way. To do this, MATLAB was used.

For every type of data file, a function was written that was able to extract the relevant data. For some types it was necessary to adjust the files manually, e.g. to remove the first and last line of data, if these were incomplete. After the data was extracted, averages were determined, which are used for further analysis.

The relevant data is stored in a structure. This is a MATLAB data type that is able to cope with data fields of different types (e.g. both alphabetic data and numerical data). The data is categorized per run, to make it easy to access the complete data set of a specific run. A graphical representation of (a part of) the structure is shown in figure 4.3.

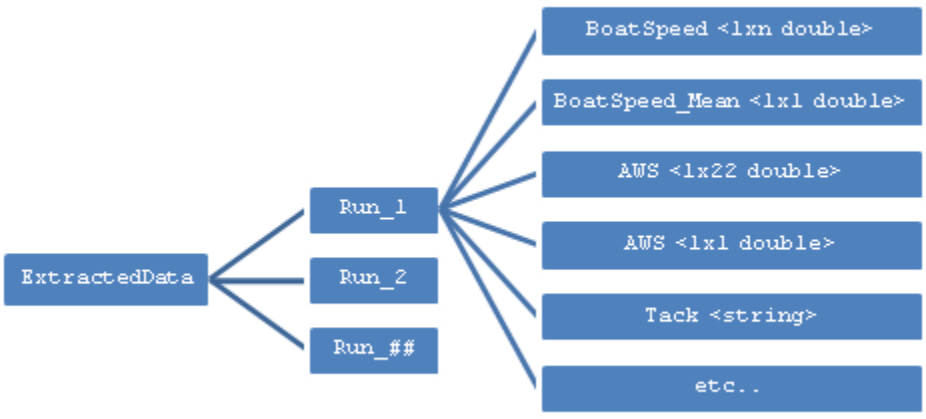

Figure 4.3: data structure.

Apparent wind angle correction

With all the data available in the structure, it was made easy to analyze it. From analyzing the apparent wind angle, as measured with the sonic anemometer followed that the average apparent wind angle on both tack differed. The average values of the apparent wind angle for heading VMG is shown in table 4.1.

Tack	Average wind angle [°]
Port	39.96
Starboard	26.91

Table 4.1: average value of apparent wind for heading VMG at both tacks.

This difference of 13.05 degrees is most likely to be caused by a misalignment of the sonic anemometer with the centre line of the yacht. To correct for this misalignment, the values of the apparent wind angle for port were lowered by the half difference, and the values for the starboard tack are increased by the half difference.

Force Evaluation via Pressures and VSPARS

To determine the driving force and the heeling moment the Force Evaluation via Pressures and VSPARS (FEPV) system is used. This method uses the VSPARS data to extrapolate the full sail shape. Using the pressure measurements on known discrete location the pressure distribution of the full sail is determined. Knowing the shape and pressure on the sail, the force distribution over the sails is determined (Le Pelley, Morris & Richards, 2012) (Morris, 2011). The determined forces are stored in an Excel sheet for further processing.

The code as developed by Morris was slightly altered to be able to cope with the input of pressure data from the data structure and the fact that the data files for the main sail consisted of position data for 5 stripes instead of the 3 stripes.

Tap position in sail

To get insight in the code plots were made which show the determined sail shape, the VPSPARS stripes and the positions of the pressure taps. These plots showed the pressure taps in the main sail lower than the VSPARS-stripes. In the head sail the pressure taps are higher. This is shown in figure 4.5. This is incorrect, since it is assumed that the pressure taps have the same height as the VSPARS stripes.

Stripe	Main sail		Head Sail	
	Height tap [mm]	Height VSPARS mm]	Height tap [mm]	Height VSPARS mm]
Top	2780	3980	3458	3127
Middle	5502	6702	6544	6101
Bottom	7690	8890	9708	9150

Table 4.2 height of VSPARS stripes and pressure taps.

The height of the taps and VSPARS stripes are tabulated in table 4.2. By analyzing the differences and the code, it can be deducted that the difference is caused by a difference between the datum that is used for the taps and the datum that is used for the VSPARS data. The code uses a datasheet to read the positions of the taps. In span wise direction these positions are given as a distance from the tack of the sail along the luff. In chord wise direction these are given as percentage of the chord. The datum is thus the tack of the sail, and the positive Z-direction is the luff.

The VSPARS software gives the x, y and z position of the stripes relative to another datum. In the case of the experiments with the Stewart 34 the datum is the aft face of the mast at deck height. The different data are shown in figure 4.4.

That the differences in height are indeed caused by a difference in coordinate system can be verified by analyzing the heights. For the main sail the difference between the height of the taps and the height of the VSPARS stripes is consequent 1200 mm. This value corresponds to the value $tackZ_{main}$, the vertical distance of the tack from the datum, which is entered in VSPARS.

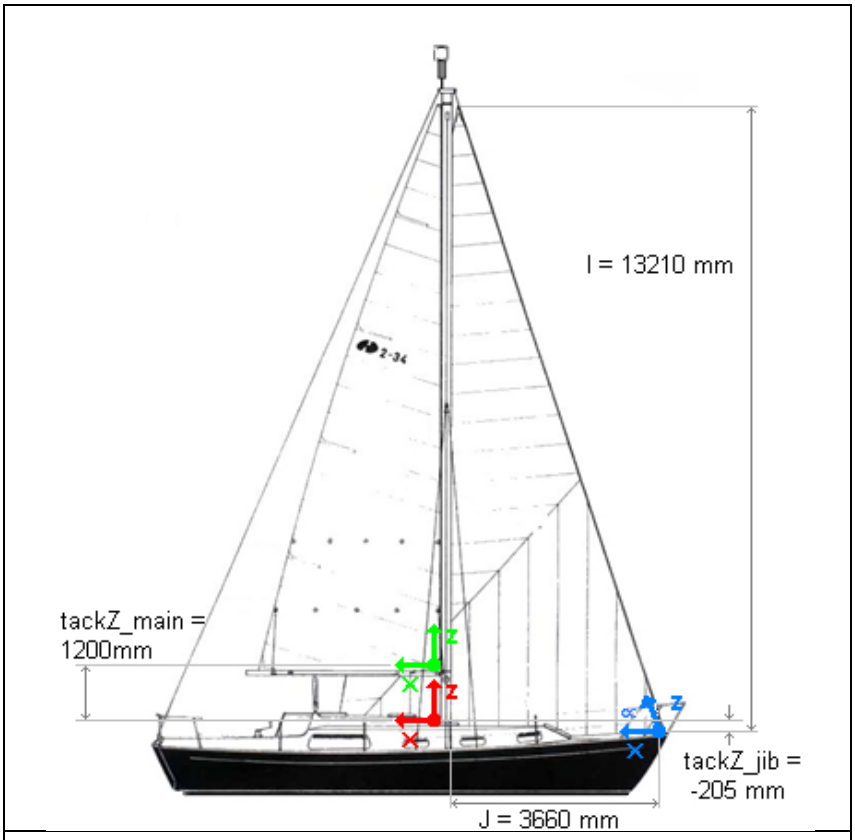

Figure 4.4: different data for VSPARS, main sail pressure and head sail pressure.

$$VSPARS\ Z_{main} = TapZ_{main} + tackZ_{main}$$

For the jib, the height of the VSPARS stripes can be expressed as a function of the tap height using the following expression:

$$VSPARS\ Z_{jib} = \left(TapZ_{jib} + tackZ_{jib}\right)\sin(\alpha)$$

Where α is given by:

$$\alpha = \tan(I/J)$$

This difference in datum has consequences for the extrapolation of pressure distribution over the sail. The pressures are extrapolated from positions that do not correspond to the position where they were measured.

The code has been checked throughout, but the code does not seem to take care of the difference in datum somewhere else. Further development of the code was beyond the scope of this project. A rough check of the consequences of the difference in datum has been performed. By adjusting the Z-coordinates of the taps in the datasheet to the Z-coordinates of the VSPARS stripes, the height of tap locations correspond to the height of the VSPARS stripes (see figure 4.6). The forces were recalculated. Differences appear to be up to 6.5%. Because the performed check was rough, the new calculated forces were not used for further analysis. It is recommended to adjust the code to be able to cope with the difference in datum, in order to get a more accurate interpolation.

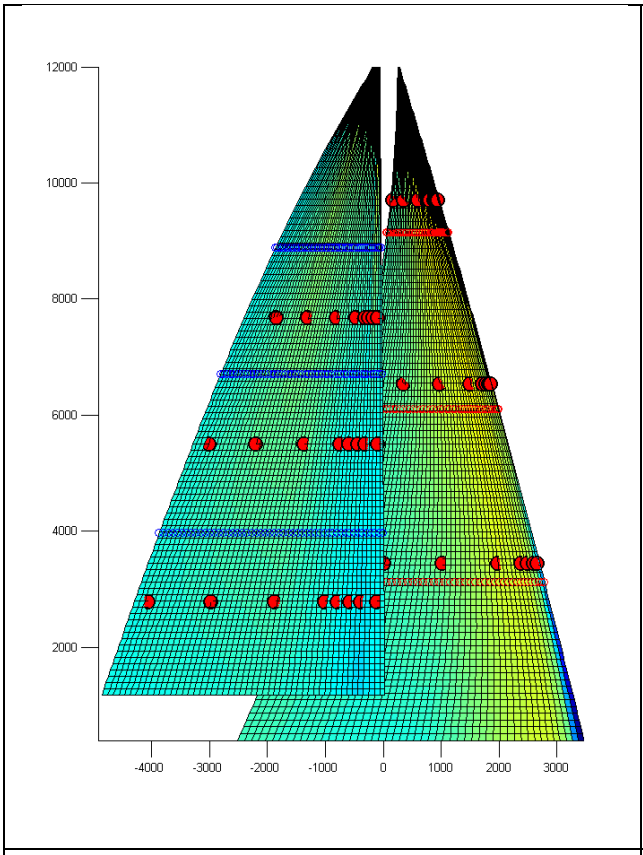

Figure 4.5: height difference between VSPARS stripes (blue and red circles) and pressure taps (red circles).

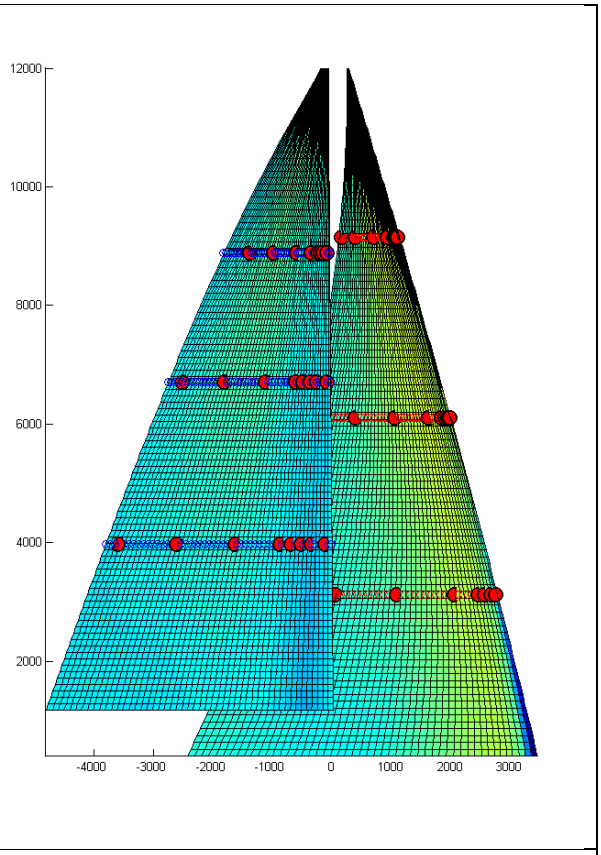

Figure 4.6: VSPARS stripes (blue and red circles) and pressure taps (red circles) placed at the same height.

Gap width

To be able to compare the gap width of the sails in different situations, the gap width has to be defined. For this case the gap width has the following definition:

"The shortest distance between the leech of the headsail and any point of the mainsail"

This gap width is determined for every run at three different heights. These are the heights of the VSPARS stripes of the jib. The algorithm uses the coordinates of the VSPARS stripes of the headsail and the extrapolated shape of the main sail. The last point of every VSPARS stripe of the head sail is determined. For each of these points the difference between this point and every point in the headsail is determined. The minimum of these distances is searched. A typical plot of the leech points and the corresponding closest points in the mainsail is shown in figure 4.7.

Performance indicators

Under ideal conditions it would be possible to compare the performance of different runs with each other. However, tests at full scale are seldom ideal. Even small variations in sea state, tide, wind speed and direction cannot be controlled at full scale. To be able to detect performance differences with different settings, it should be possible to compare the performance. For that reason performance indicators are used. These indicators give the performance corrected for the effect of variations in wind speed and direction. The performance indicators are calculated using Excel. How they are determined is described below.

The driving force is the component of the aerodynamic force in the longitudinal direction of the yacht. Since the apparent wind angle (AWA) differs for every run, this needs to be corrected. This means that the component of the driving force in the direction of the wind is regarded, this is called 'Force Made Good' (compare: Velocity Made Good). To correct for the change in wind speed, the driving force is divided by the dynamic pressure $\frac{1}{2}\rho_{air}v^2$. Because the density of the air is assumed to be constant over the day, the division by ρ_{air} is omitted. This gives the following expression:

$$CF_{x,MG} = \frac{F_x}{\frac{1}{2}v^2}\cos(AWA) = \frac{F_x}{\frac{1}{2}AWS^2}\cos(AWA)$$

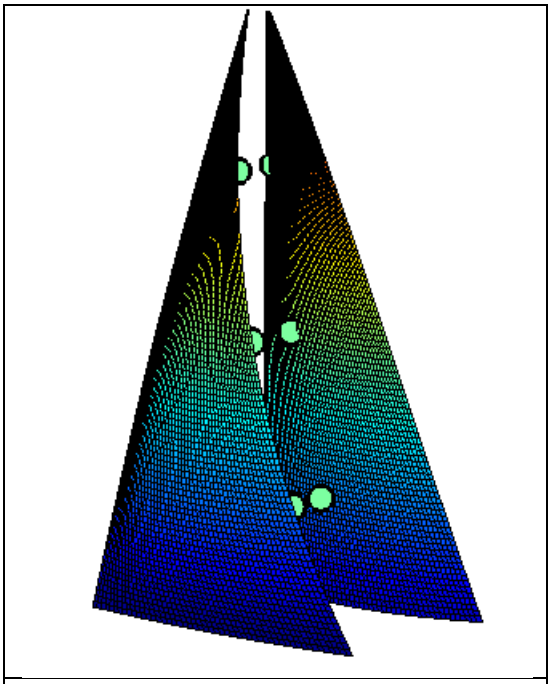

Figure 4.7: Leech points of the head sail and their corresponding closest points in the main sail

The values of $CF_{x,MG}$ is plotted against AWA (see figure 4.8). Both tacks are distinguished because there is a big difference between the two of them. The cause of this asymmetry is not fully understood, but could be caused by the extrapolation method of the pressure distribution, the different definitions of standard trim at both tacks, or the fact that the pressure taps are stuck to one side of the sail.

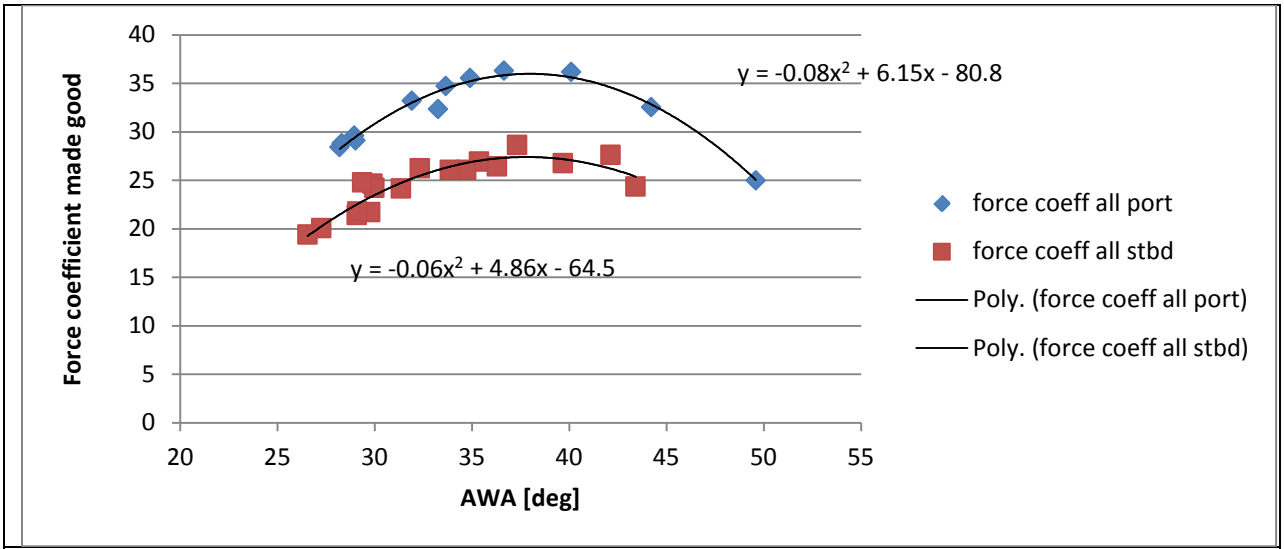

Figure 4.8 force coefficient made good vs. Apparent Wind Angle.

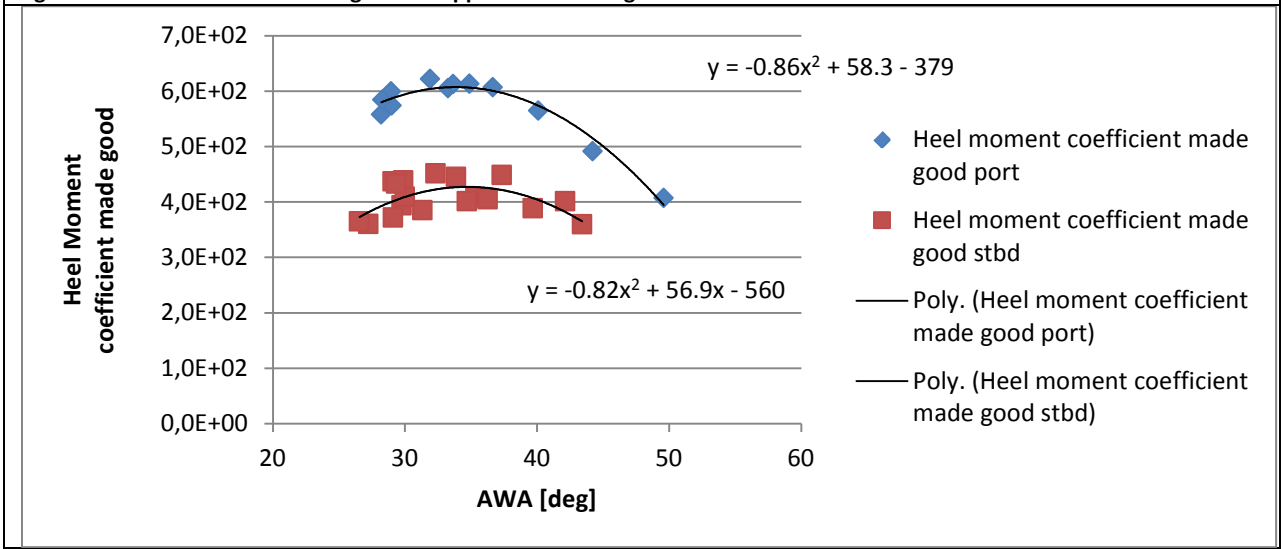

Figure 4.9 heel moment coefficient made good vs. Apparent Wind Angle.

What can be seen from the trend is that there is still a variation with the AWA. This is as expected. The sails are trimmed to perform optimal for a heading called VMG, which is in the middle of the AWA range. For the experiments in which is deflected from this heading, the sails are trimmed suboptimal so the performance decreases. To take account for this effect a correction is applied. The runs are corrected to a standard AWA, designated by η. The expressions for the trend line are used for this. The functions for the trend lines are:

$$CF_{x,MG,port}(AWA) = -0.08 \cdot AWA^2 + 6.15 \cdot AWA - 80.8$$
$$CF_{x,MG,starboard}(AWA) = -0.06 \cdot AWA^2 + 4.86 \cdot AWA - 64.5$$

The measured value of the force made good coefficient $CF_{x,MG}$ is corrected by subtracting the value for the force made good coefficient as calculated by the trend line for that specific apparent wind angle. This gives the difference between the measured value and the trend line. To correct the force made good coefficient, the value of the force made good coefficient at the angle η is added:

$$CF_{x,MG,\eta} = CF_{x,MG} - CF_{x,MG}(AWA) + CF_{x,MG}(\eta)$$

To determine the heel moment made good coefficient the same procedure is applied. The plot of the heel moment made good vs. AWA is shown in figure 4.9. The trend lines are given by:

$$CM_{x,MG,port}(AWA) = -0.86 \cdot AWA^2 + 58.3 \cdot AWA - 379$$
$$CM_{x,MG,starboard}(AWA) = -0.82 \cdot AWA^2 + 56.9 \cdot AWA - 560$$

The corrected heel moment made good is given by:

$$CM_{x,MG,\eta} = CM_{x,MG} - CM_{x,MG}(AWA) + CM_{x,MG}(\eta)$$

The angle η depends on the heading of a run. The choice of the value of η is based on a rounded average value of AWA for each of the three headings, and is tabulated in table 4.3.

Heading	η [°]
Pinching	29
VMG	33
Footing	40

Table 4.3: Standard angle for different headings

5. Results

In this chapter the results are presented. The data is processed as described in the previous chapter.

For every run the values of the following quantities are tabulated in appendix A.

- Cap shroud position (D)
- Apparent wind angle (AWA)
- Apparent wind speed (AWS)
- Boat speed (V_s)
- Driving force (F_x)
- Corrected driving force made good coefficient ($CF_{x,MG,\eta}$)
- Heeling moment (M_x)
- Corrected Heeling moment made good coefficient ($CM_{x,MG,\eta}$)

The table includes an overview of the settings that were applied to the specific run. Run number 1, 2, 22 and 24 are not shown because these were either zero runs or runs with corrupted data.

A rough check of the correctness of the driving force and heeling force is performed. Using driving force coefficients from literature the driving force is determined. This is compared to the determined driving force. The driving force is determined for a wind speed of 8.5 m/s and an apparent wind angle of 33 degrees. This gives a driving force coefficient C_M of 0.62 (Fossati, 2007). The driving force is determined using the following expression:

$$F = \frac{1}{2} \cdot \rho_{air} \cdot AWS^2 \cdot SA \cdot C_M$$

With a sail area SA of 62 m^2 and an air density ρ_{air} of 1.25 kg/m^3 this gives a driving force of approximately $1.7 \cdot 10^3$ N. This is slightly higher than the measured values for the driving force, but deviates not too much. The difference might be explained by the fact that the used driving force coefficient is for a more modern rig.

5.1 First hypothesis: boat speed V_S

The first hypothesis is:

Yachts of the type Stewart 34 are able to sail faster upwind with slack cap shrouds.

In figure 5.1-2 the boat speed is shown for various settings of the shroud position. For the runs on the port tack a minimum boat speed is achieved for the medium to slack shroud setting. The boat speed increases when the shrouds are eased or tightened. This can be seen for all three headings. On the starboard tack however, a maximum boat speed is achieved for the medium to slack shroud setting. This trend shows as well for all three headings.

The difference between the trends at the two tacks can be caused by effects that are not corrected for when regarding boat speed, such as different wind speed or sea state. That the headings show similar trends can be explained by the order of the experiments. First the experiments for all three runs on a

certain shroud setting are done. After that the shroud setting is adjusted. That means that experiments on similar shroud settings are performed with little time in between, sometimes less than a minute. The conditions under which these experiments are performed are thus similar. This causes similar trends over the shroud settings.

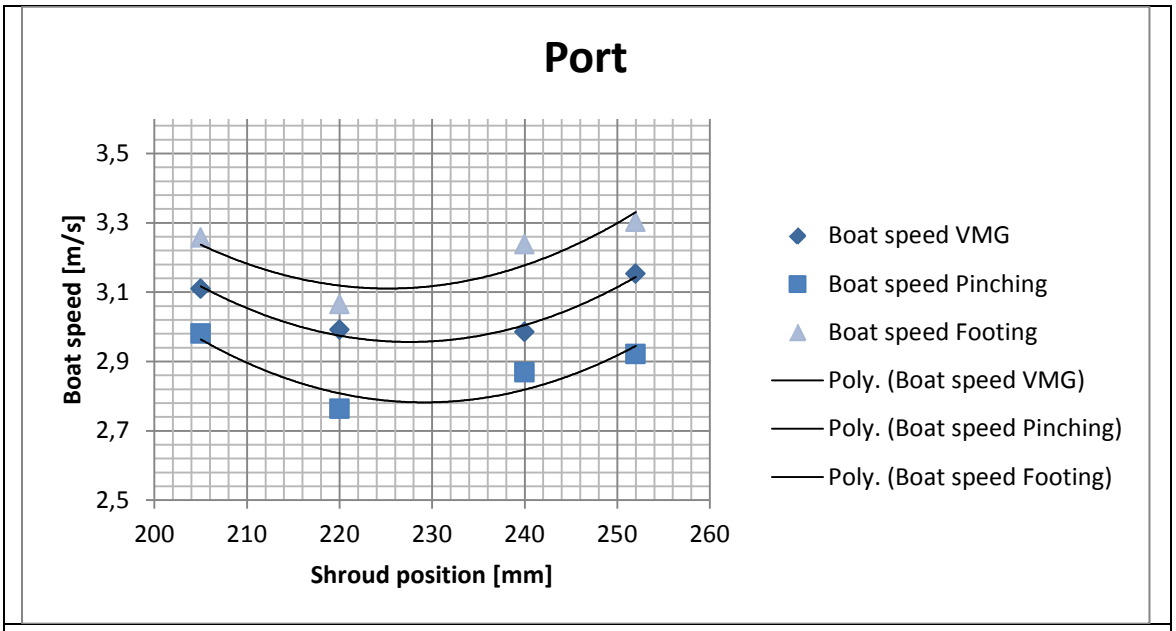

Figure 5.1: boat speed vs. shroud position on port tack for various headings.

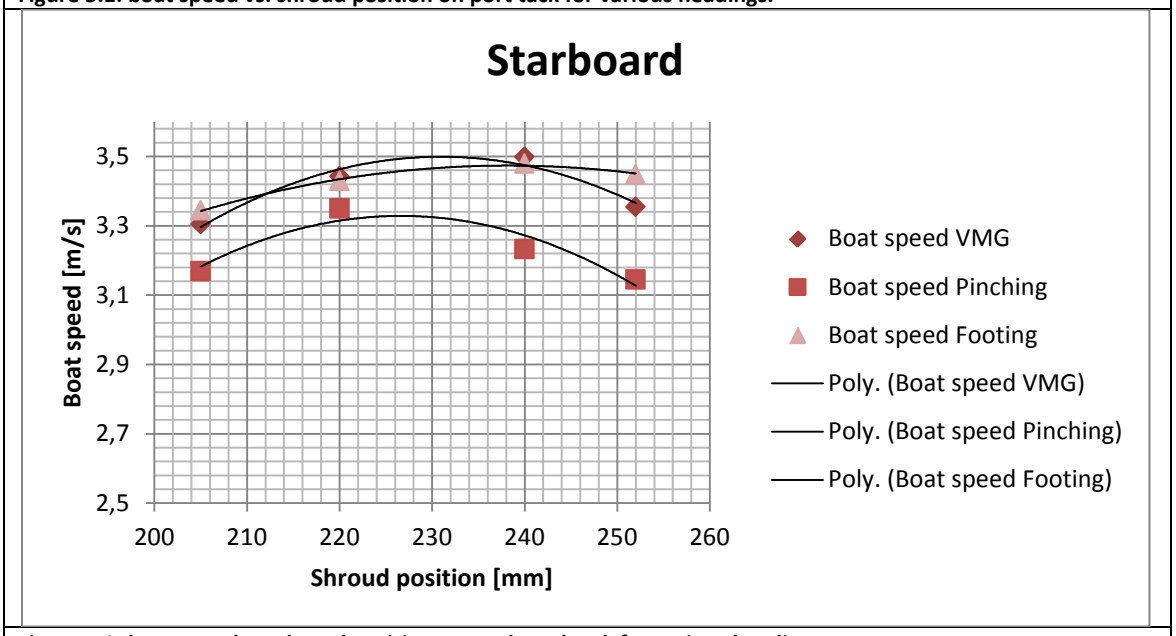

Figure 5.2: boat speed vs. shroud position on starboard tack for various headings.

5.2 Second hypothesis: Apparent Wind Angle

The second hypothesis is:

Yachts of the type Stewart 34 are able to sail closer to the wind with slack cap shrouds.

In figure 5.3-4 the apparent wind angle is shown for various settings of the shroud position. A clear trend is hard to distinguish. For every run the course to steer had to be found again. Variations in the idea of the optimal course might be bigger than the small variations of apparent wind angle with shroud tension, making it hard to distinguish a trend without correcting for these variations

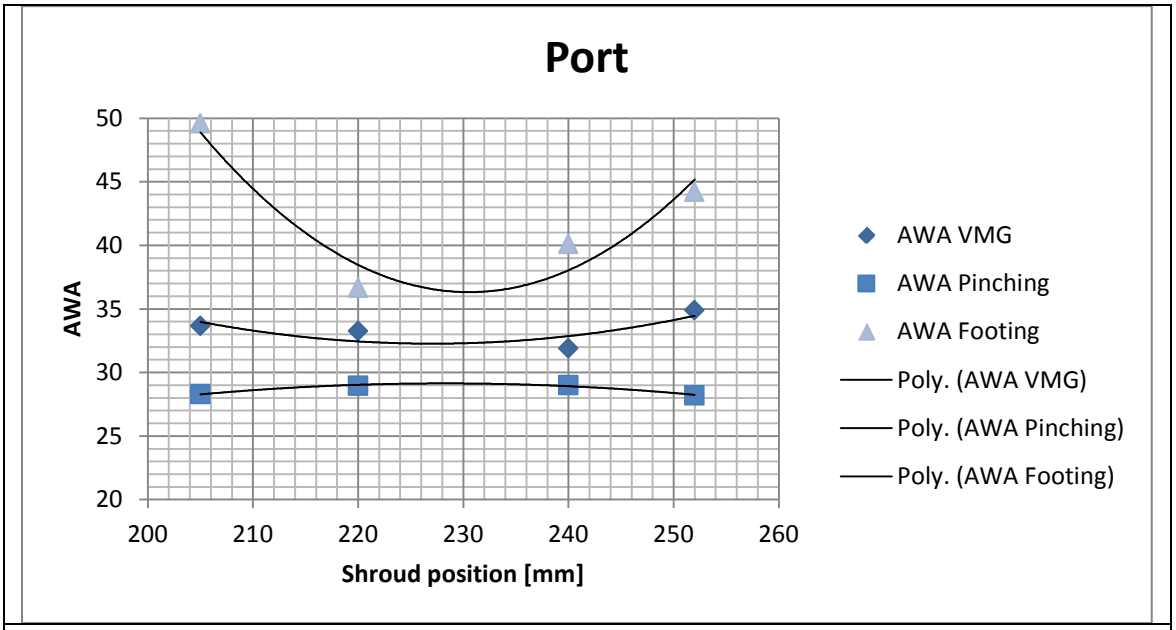

Figure 5.3: Apparent Wind Angle (AWA) vs. shroud position on port tack for various headings.

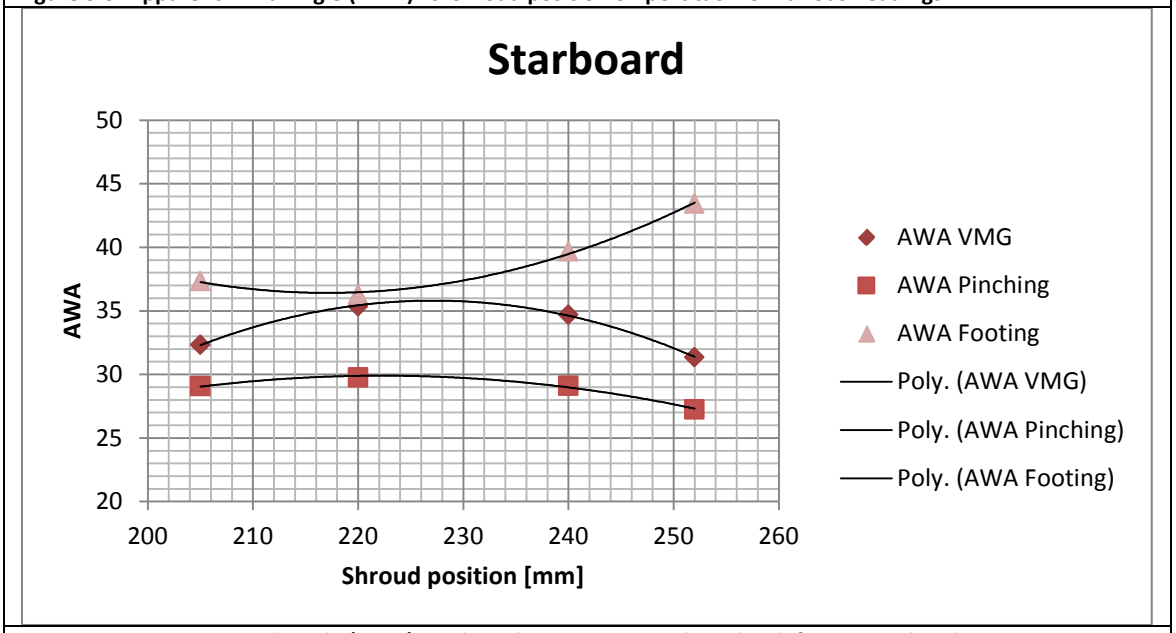

Figure 5.4: Apparent Wind Angle (AWA) vs. shroud position on starboard tack for various headings.

5.3 Third hypothesis: corrected force made good coefficient $CF_{x,MG,\eta}$

The third hypothesis is:

Yachts of the type Stewart 34 are able to achieve a higher $CF_{x,MG,\eta}$ with slack cap shrouds.

In figure 5.5-7 the corrected force made good coefficients are shown for different shroud settings. The differences in force coefficient between port an starboard are not fully understood, but might be due to asymmetry in sail trim, the fact that the pressure taps are applied to one side of the sail instead of symmetrical or by an error in the zero readings of the pressure taps. There are no clear trends of the corrected force coefficient with variation of the shroud position. This might be due to the fact that an increased force coefficient not necessarily implies an increased performance. If the heel moment increases with the force coefficient, the heel angle increases and the hydrodynamic drag increases.

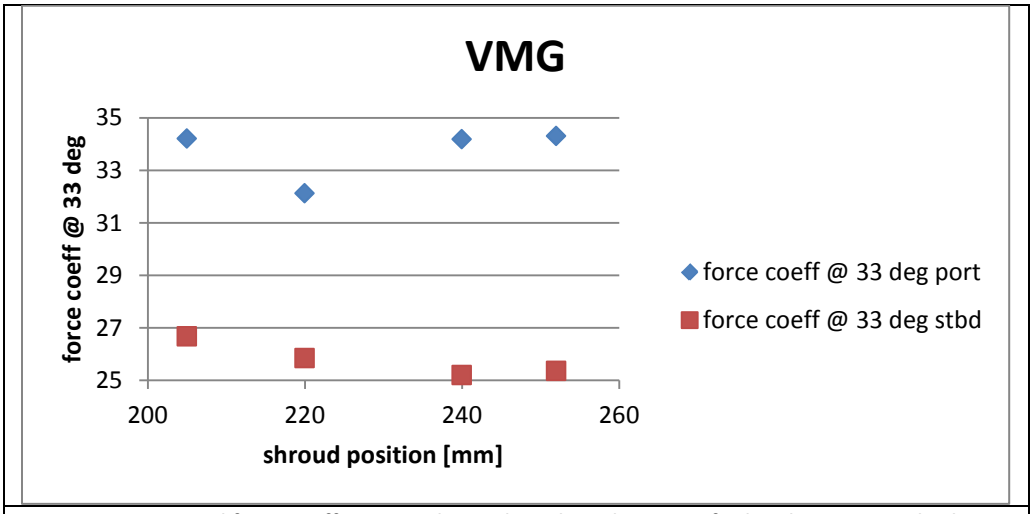

Figure 5.5: Corrected force coefficient made good vs. shroud position for heading VMG on both tacks.

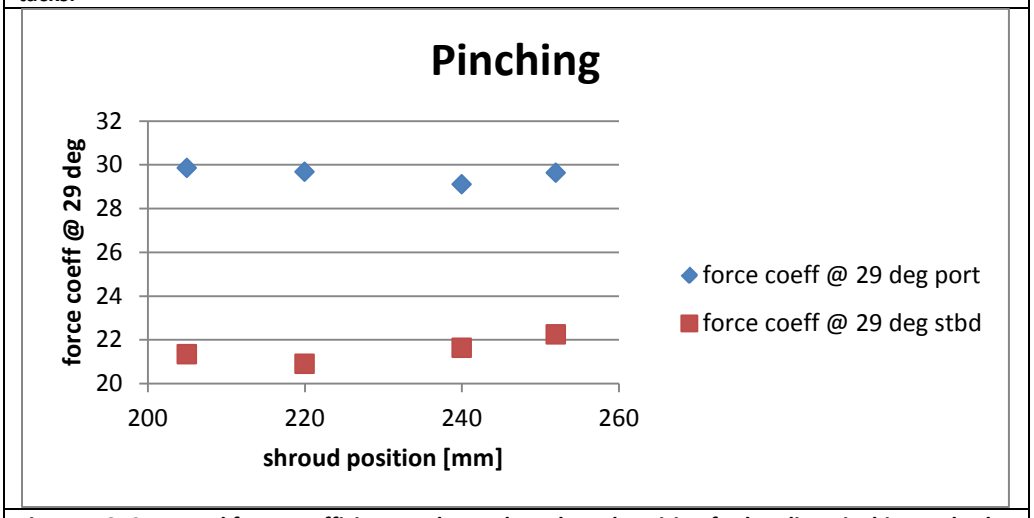

Figure 5.6: Corrected force coefficient made good vs. shroud position for heading pinching on both tacks.

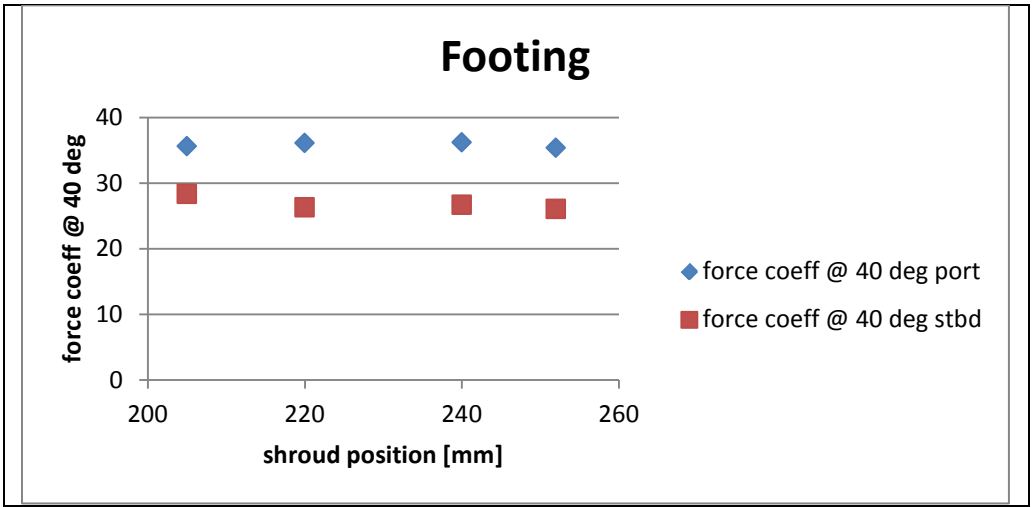

Figure 5.7: Corrected force coefficient made good vs. shroud position for heading footing on both tacks.

5.4 Fourth hypothesis: drive over heel $\frac{CF_{x,MG,\eta}}{CM_{x,MG,\eta}}$

The fourth hypothesis is:

Yachts of the type Stewart 34 are able to achieve a higher $\frac{CF_{x,MG,\eta}}{CM_{x,MG,\eta}}$ with slack cap shrouds.

In figure 5.8-10 the force made good coefficient over corrected heel moment made good coefficient is shown for different shroud settings. In all cases but for VMG on port, a similar trend can be seen. The value of $\frac{CF_{x,MG,\eta}}{CM_{x,MG,\eta}}$ has a maximum for a shroud position which corresponds to the medium to slack setting. This can be regarded as the optimum shroud setting, because this is the setting where $CF_{x,MG,\eta}$ is maximal for minimal $CM_{x,MG,\eta}$.

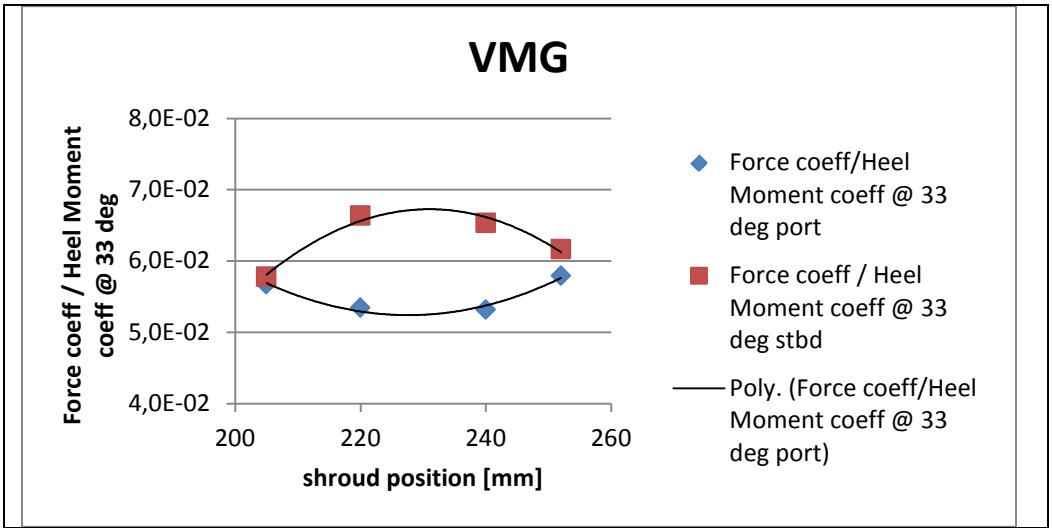

Figure 5.8: Corrected force coefficient made good over correct heel moment coefficient vs. shroud position for heading VMG on both tacks.

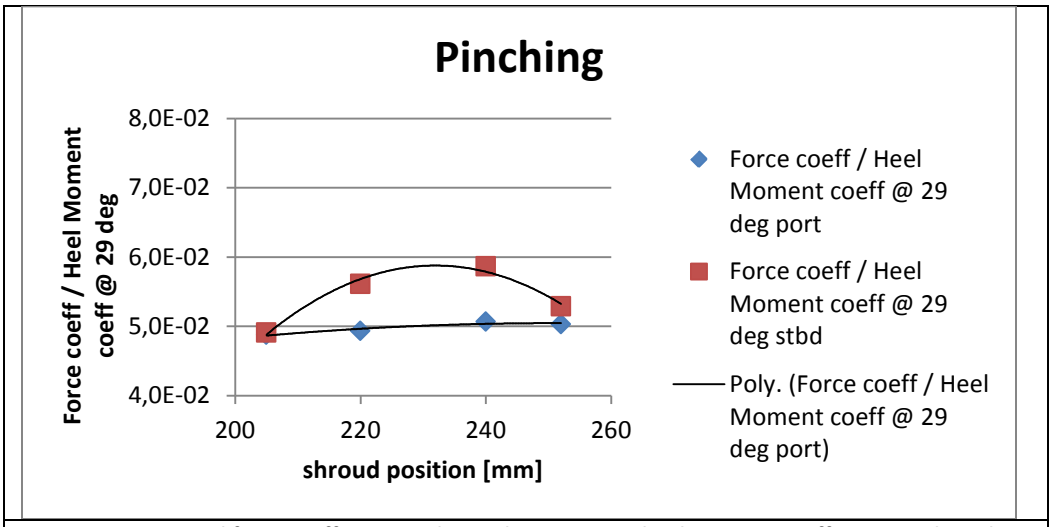

Figure 5.9: Corrected force coefficient made good over correct heel moment coefficient vs. shroud position for heading VMG on both tacks.

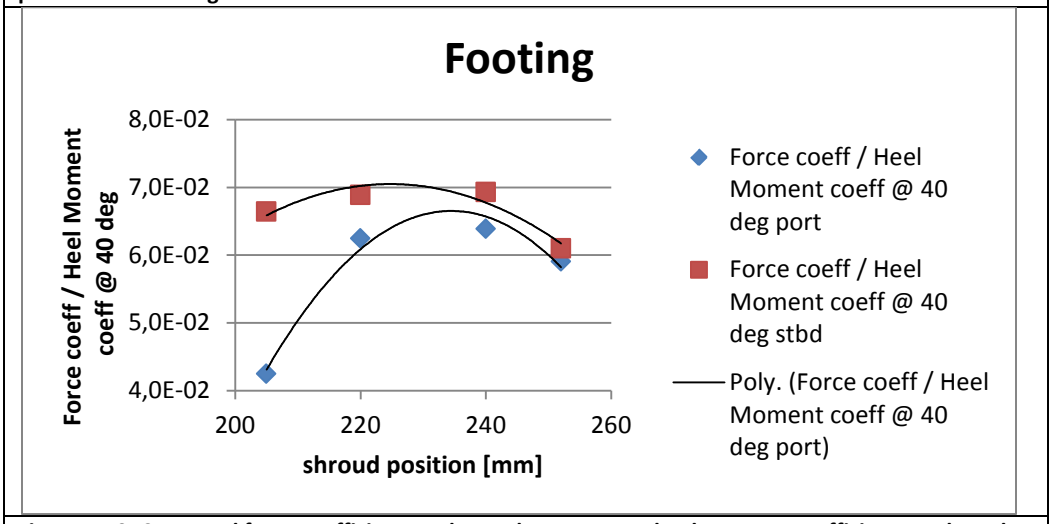

Figure 5.10: Corrected force coefficient made good over correct heel moment coefficient vs. shroud position for heading VMG on both tacks.

5.5 Fifth hypothesis: mast sag

The fifth hypothesis is:

The sag of the mast top of a Stewart 34 increases with increasing slack cap shrouds.

In figure 5.11-16 sag of the mast is shown for different shroud settings. On the vertical axis the height above the datum is shown, on the horizontal axis the deflection from the neutral position of the mast. For all three headings and both tacks the sideways mast deflection increases with increasing slackness of the cap shroud. This is the expected behaviour. It should be noted that the defection at an approximate height of 6700 mm is constant. This is the height of the spreaders. The D1 shrouds keep prevent the mast at this position from deflecting.

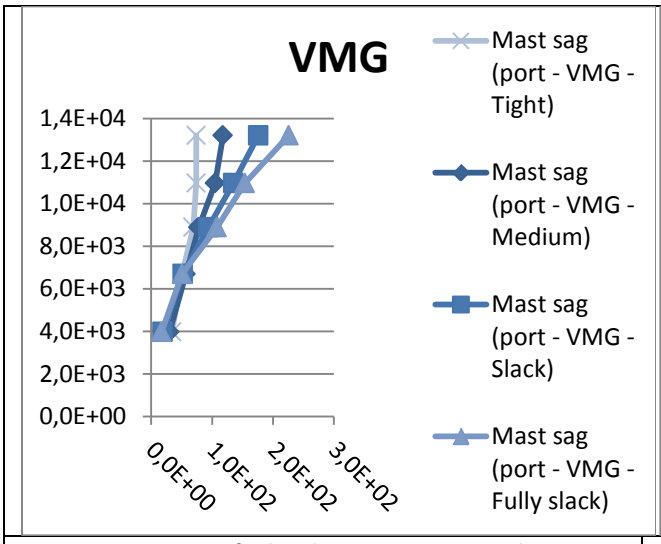

Figure 5.11: mast sag for heading VMG on port tack.

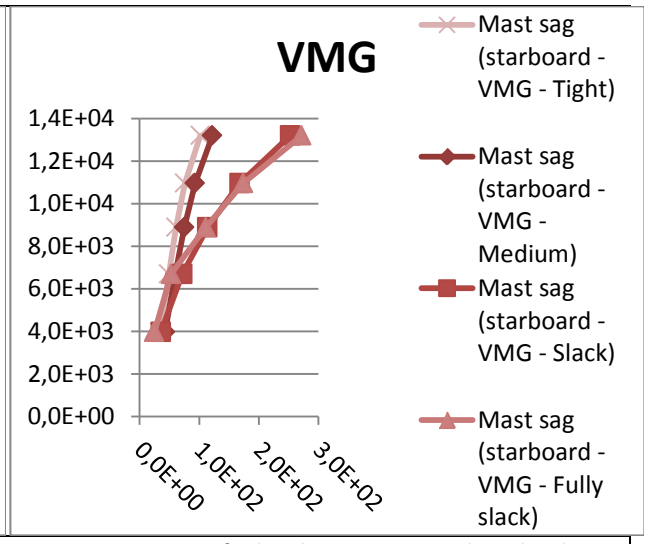

Figure 5.12: mast sag for heading VMG on starboard tack.

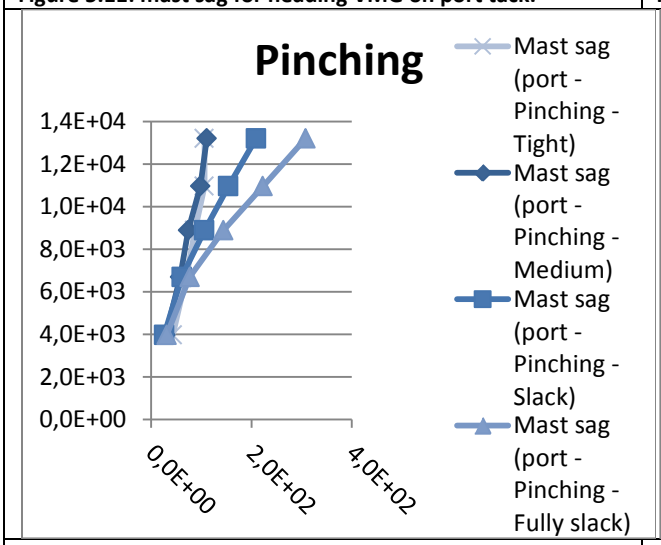

Figure 5.13: mast sag for heading pinching on port tack.

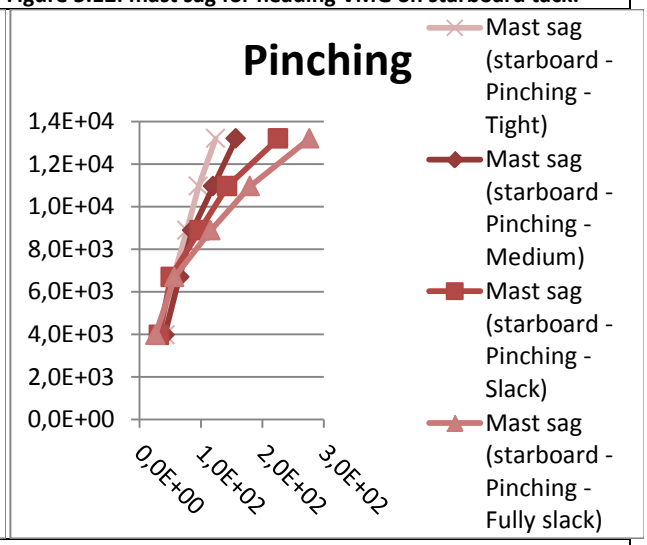

Figure 5.14: mast sag for heading pinching on starboard tack.

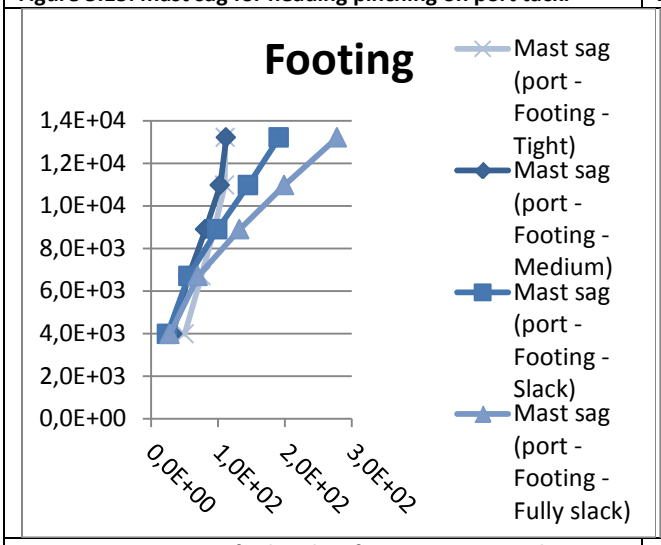

Figure 5.15: mast sag for heading footing on port tack.

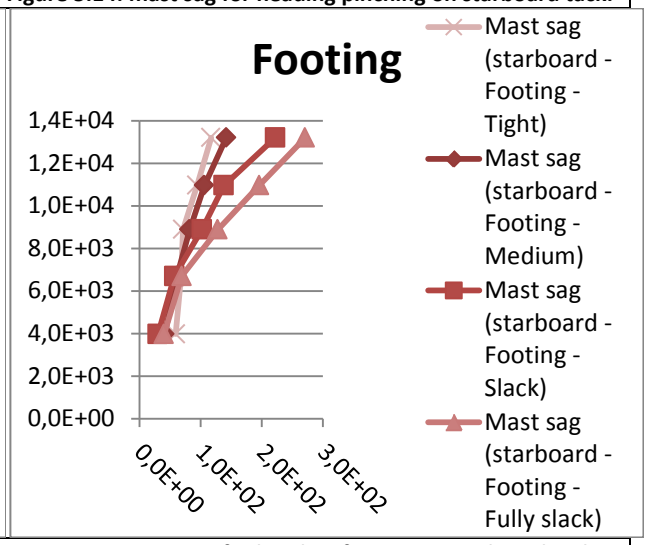

Figure 5.16: mast sag for heading footing on starboard tack.

5.6 Sixth hypothesis: Gap width

The sixth hypothesis is:

The gap width of a Stewart 34 increases with increasing slack cap shrouds.

In figure 5.17-5.22 gap width is shown for different shroud settings. The gap width is given at three different heights. What is interesting to see is that the trends of the gap width at different heights usually follow the same pattern. The gap width is minimal for the medium shroud setting. It increases with increasing shroud length, which is what is expected. However, the gap width also increases if the cap shroud setting is tight. This phenomenon is not fully understood. What should be noticed as well is the difference in gap width between the port and starboard tack. This might be caused by the fact that the standard trim for both tacks was defined different.

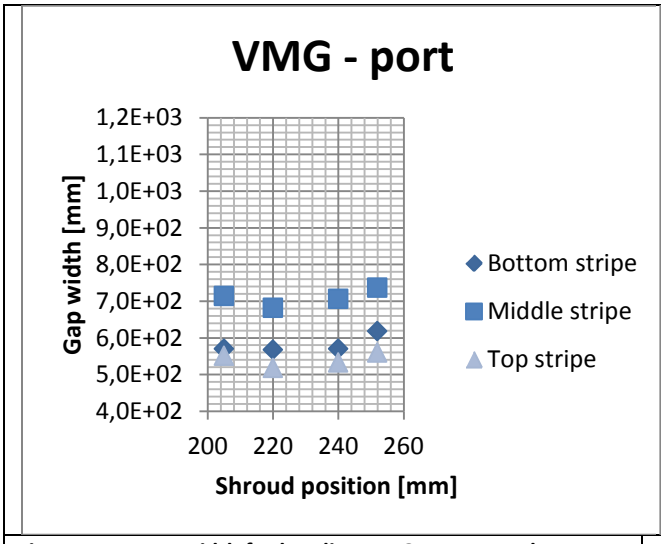

Figure 5.17: gap width for heading VMG on port tack.

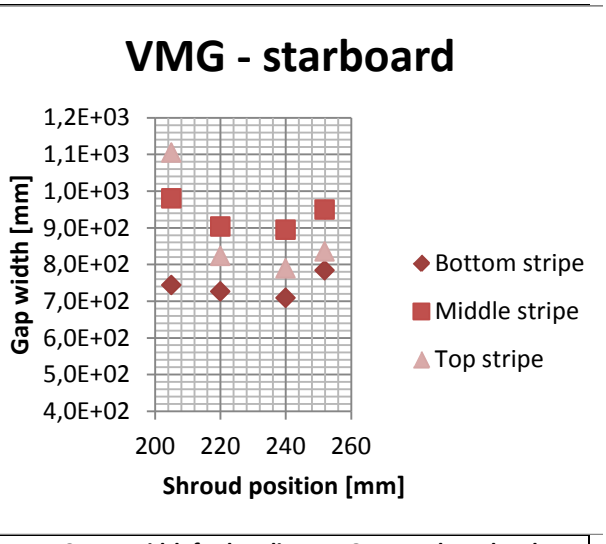

Figure 5.18: gap width for heading VMG on starboard tack.

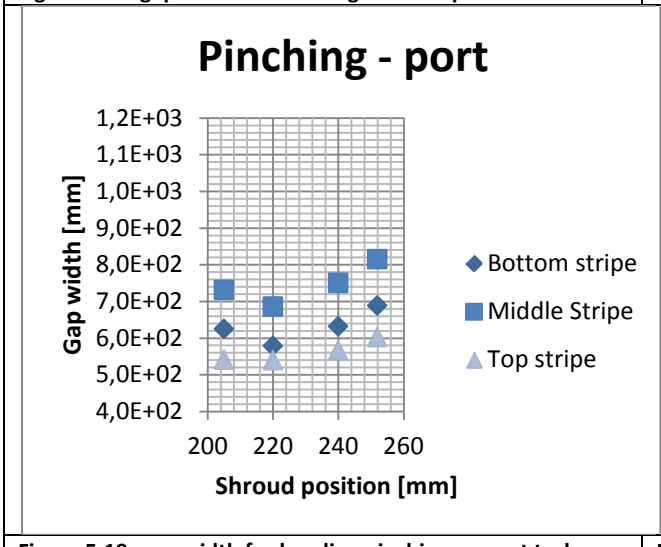

Figure 5.19: gap width for heading pinching on port tack.

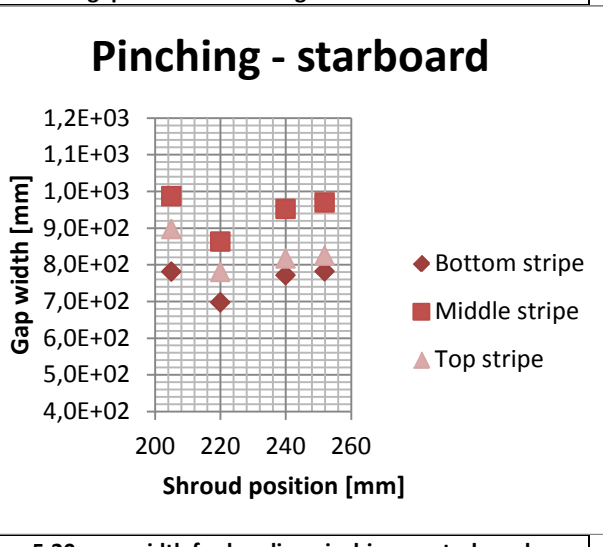

Figure 5.20: gap width for heading pinching on starboard tack.

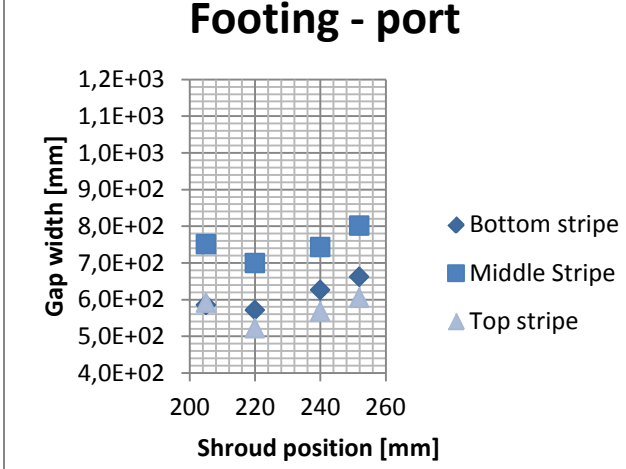

Figure 5.21: gap width for heading footing on port tack.

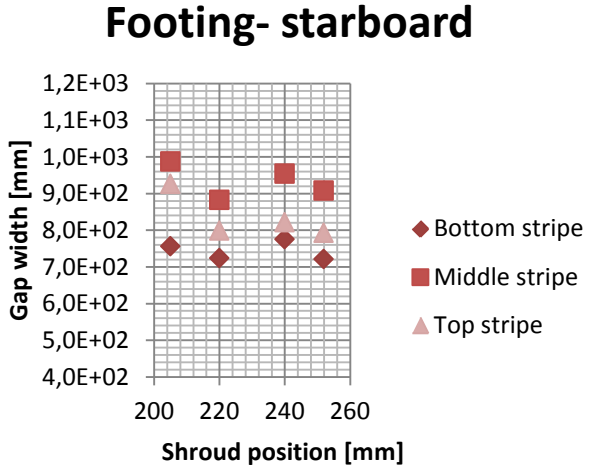

Figure 5.22: gap width for heading footing on starboard tack.

5.7 Seventh hypothesis: corrected driving force made good coefficient and gap width

The seventh hypothesis is:

Yachts of the type Stewart 34 are able to achieve a higher $CF_{x,MG,\eta}$ with a bigger gap width.

The corrected driving force made good coefficient is shown for different conditions in figure 5.5-7. The gap width is shown for the same conditions in figure 5.17-22. The trends of gap width with shroud position seem to have similarities with the trends of corrected driving force coefficient with shroud position. For most combinations of tack and heading this seems to be the case. Exceptions are pinching on port tack and footing on port tack. To confirm these similarities in trend the corrected driving force coefficient is plotted as a function of the gap width for different combinations of tack and heading in figure 5.23. Here we can see again, that for most cases $CF_{x,MG,\eta}$ seems to increase with increasing gap width.

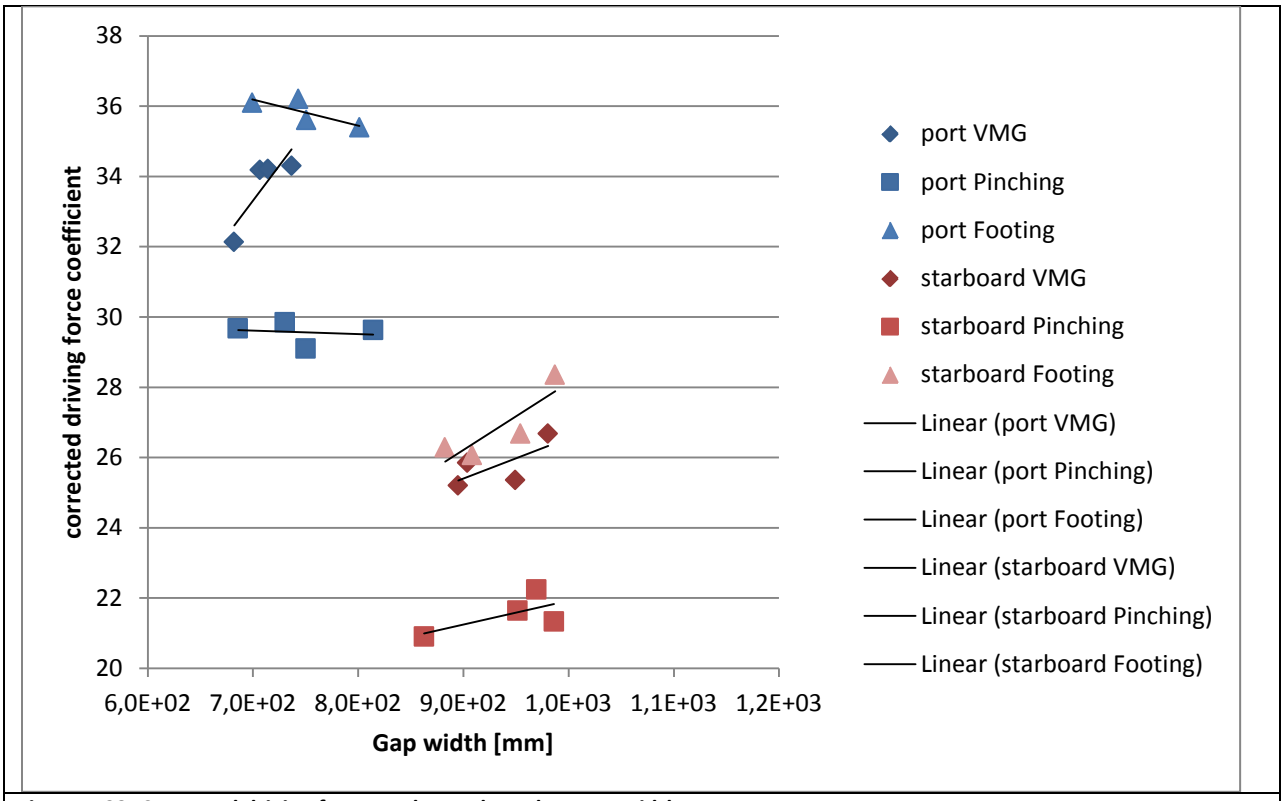

Figure 5.23: Corrected driving force made good good vs. gap width.

6. Conclusions and recommendations

In this chapter the conclusions that follow from these results will be presented. Recommendations for further research on the effect of rig tension on the performance of the Stewart 34 and the FEPV system will be given.

6.1 Conclusions

- From the experiments a good set of data was acquired. The determined driving forces conform reasonably well to theoretical values. Asymmetry in the data was found.
- Performance indicators such as boat speed and angle to the wind proved to be hard to compare, due to variations in conditions and yacht attitude which are inevitable for full scale tests. Normalization with wind direction and speed was required.
- The value of $\frac{CF_{x,MG,\eta}}{CM_{x,MG,\eta}}$ maximizes for most combinations of tack and heading at a rig setting between medium and slack. And exception is shown in the measurements on port tack while heading for maximum VMG.
- The fall off of the mast top clearly increases with slacker cap shrouds. This is shown for all combinations of tack and heading.
- The gap width has a minimum for the medium shroud setting. As expected the gap width increases with increasing slackness of the shrouds. However the gap width also increases when the cap shrouds are set to tight.
- For four out of six cases it is shown that the corrected driving force made good increases with increasing gap width. This indicates that there might be an increase in performance associated with an increase in gap width.

6.2 Recommendations

- Further investigation in the cause of the asymmetry of the data is required. The asymmetry might be caused by:
    - Different standard trim definitions between the two tacks.
    - Interference by the pressure taps.
    - A bias in the zero readings for the pressure taps.
- Further investigation in the possibilities to improve the extrapolation algorithm of the pressure distribution is recommended.
- Effort should be made to make the different test runs better comparable, e.g. by making the standard trim settings more equal.
- Determining the cause of the trend of the gap width with shroud tension is recommended. Improvement of the definition of the gap width might be possible.
- Further research to the behaviour of the performance indicators with variations of the gap width is required to fully understand the behaviour.

Bibliography

Le Pelley, D., Morris, D., Richards, P., (2012). *Aerodynamic force deduction on yacht sails using pressure and shape measurements in real time.* 4th HPYD conference, Auckland 2012

Gentry, A. (2006). *The Origins of Lift*. as retrieved 20th of December 2011 from http://www.arvelgentry.com/techs/origins_of_lift.pdf

Fossati, F. (2007). *Aero-hydrodynamics and the performance of sailing yachts*. London: Adlard Coles Nautical

Gentry, A (1973) More on the Slot Effect. *SAIL Magazine*, August 1973

LINZ (2011). *Land information New Zealand tide predictions*. As retrieved 13th of February 2012 from http://www.linz.govt.nz/hydro/tidal-info/tide-tables

Marchaj, C.A. (1964). *Sailing theory and practice.* London; Adlard Coles Limited

Morris, D., (2011). *Derivation of Forces on a Sail using Pressure and Shape Measurements in Full-Scale*. Master Thesis, University of Auckland

Appendix A

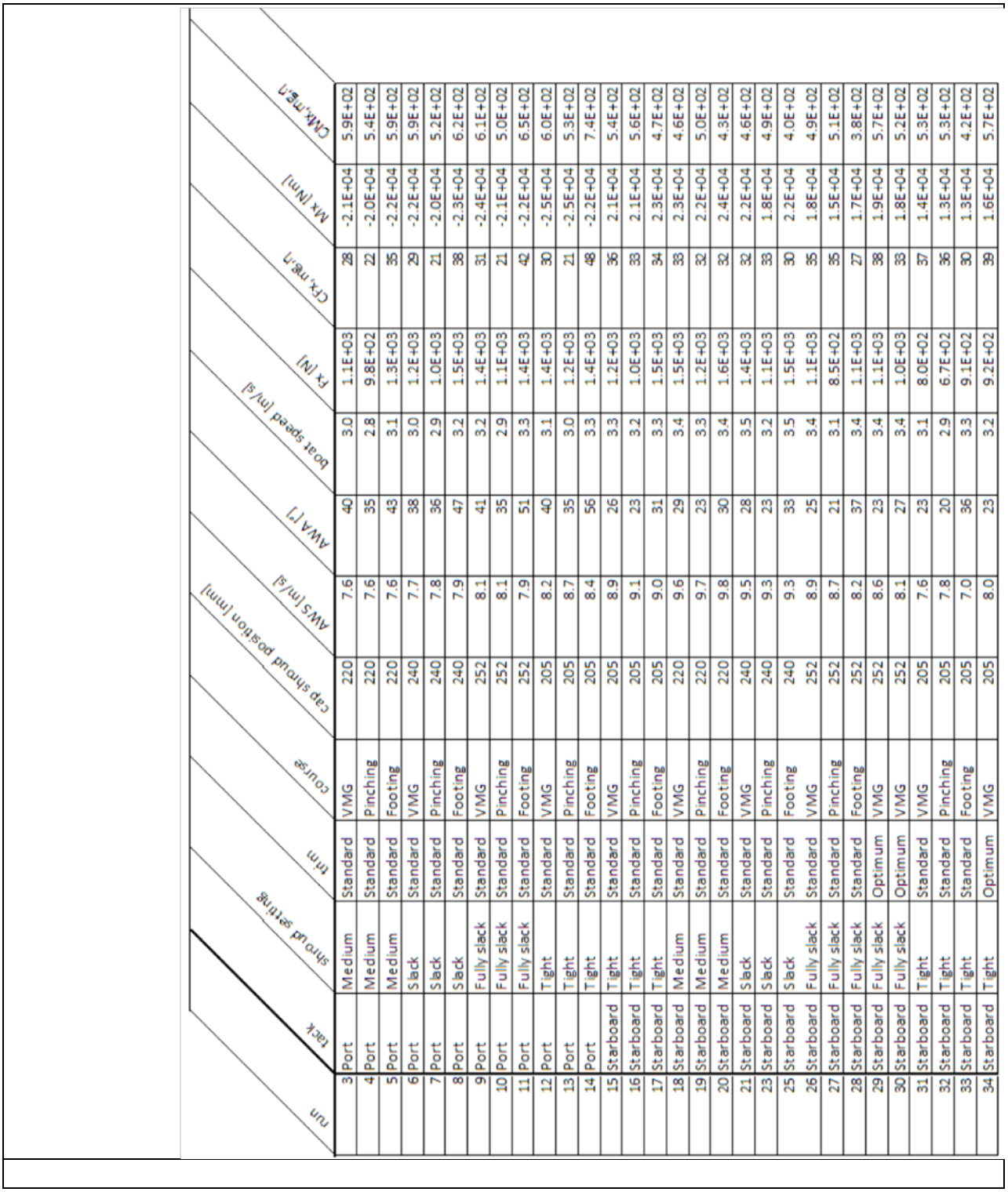

run	tack	should settings	trim	course	cap should position [mm]	AWS [m/s]	AWA [°]	boat speed [m/s]	Fx [N]	CFx,meas	MMx [Nm]	CMx,meas
3	Port	Medium	Standard	VMG	220	7.6	40	3.0	1.1E+03	28	-2.1E+04	5.9E+02
4	Port	Medium	Standard	Pinching	220	7.6	35	2.8	9.8E+02	22	-2.0E+04	5.4E+02
5	Port	Medium	Standard	Footing	220	7.6	43	3.1	1.3E+03	35	-2.2E+04	5.9E+02
6	Port	Slack	Standard	VMG	240	7.7	38	3.0	1.2E+03	29	-2.2E+04	5.9E+02
7	Port	Slack	Standard	Pinching	240	7.8	36	2.9	1.0E+03	21	-2.0E+04	5.2E+02
8	Port	Slack	Standard	Footing	240	7.9	47	3.2	1.5E+03	38	-2.3E+04	6.2E+02
9	Port	Fully slack	Standard	VMG	252	8.1	41	3.2	1.4E+03	31	-2.4E+04	6.1E+02
10	Port	Fully slack	Standard	Pinching	252	8.1	35	2.9	1.1E+03	21	-2.1E+04	5.0E+02
11	Port	Fully slack	Standard	Footing	252	7.9	51	3.3	1.4E+03	42	-2.2E+04	6.5E+02
12	Port	Tight	Standard	VMG	205	8.2	40	3.1	1.4E+03	30	-2.5E+04	6.0E+02
13	Port	Tight	Standard	Pinching	205	8.7	35	3.0	1.2E+03	21	-2.5E+04	5.3E+02
14	Port	Tight	Standard	Footing	205	8.4	56	3.3	1.4E+03	48	-2.2E+04	7.4E+02
15	Starboard	Tight	Standard	VMG	205	8.9	26	3.3	1.2E+03	36	2.1E+04	5.4E+02
16	Starboard	Tight	Standard	Pinching	205	9.1	23	3.2	1.0E+03	33	2.1E+04	5.6E+02
17	Starboard	Tight	Standard	Footing	205	9.0	31	3.3	1.5E+03	34	2.3E+04	4.7E+02
18	Starboard	Medium	Standard	VMG	220	9.6	29	3.4	1.5E+03	33	2.3E+04	4.6E+02
19	Starboard	Medium	Standard	Pinching	220	9.7	23	3.3	1.2E+03	32	2.2E+04	5.0E+02
20	Starboard	Medium	Standard	Footing	220	9.8	30	3.4	1.6E+03	32	2.4E+04	4.3E+02
21	Starboard	Slack	Standard	VMG	240	9.5	28	3.5	1.4E+03	32	2.2E+04	4.6E+02
23	Starboard	Slack	Standard	Pinching	240	9.3	23	3.2	1.1E+03	33	1.8E+04	4.9E+02
25	Starboard	Slack	Standard	Footing	240	9.3	33	3.5	1.5E+03	30	2.2E+04	4.0E+02
26	Starboard	Fully slack	Standard	VMG	252	8.9	25	3.4	1.1E+03	35	1.8E+04	4.9E+02
27	Starboard	Fully slack	Standard	Pinching	252	8.7	21	3.1	8.5E+02	35	1.5E+04	5.1E+02
28	Starboard	Fully slack	Standard	Footing	252	8.2	37	3.4	1.1E+03	27	1.7E+04	3.8E+02
29	Starboard	Fully slack	Optimum	VMG	252	8.6	23	3.4	1.1E+03	38	1.9E+04	5.7E+02
30	Starboard	Fully slack	Optimum	VMG	252	8.1	27	3.4	1.0E+03	33	1.8E+04	5.2E+02
31	Starboard	Tight	Standard	VMG	205	7.6	23	3.1	8.0E+02	37	1.4E+04	5.3E+02
32	Starboard	Tight	Standard	Pinching	205	7.8	20	2.9	6.7E+02	36	1.3E+04	5.3E+02
33	Starboard	Tight	Standard	Footing	205	7.0	36	3.3	9.1E+02	30	1.3E+04	4.2E+02
34	Starboard	Tight	Optimum	VMG	205	8.0	23	3.2	9.2E+02	39	1.6E+04	5.7E+02